Supplementary Information (SI)

A ruthenium(II) polypyridyl complex as a luminescent chemodosimetric probe for selective and sensitive detection of phosgene and nerve agent simulant

Juhi Sayala,[a] Nitin Shukla[a] and Ashis K. Patra*[a]

[a] Department of Chemistry, Indian Institute of Technology Kanpur, Kanpur 208016, Uttar Pradesh, India, E-mail: akpatra@iitk.ac.in

Contents	**Page**
Fig. S1 Structures of ruthenium(II) complexes [**1**]-[**3**] studied in this work.	**4**
Fig. S2 ESI-MS spectrum of complex [**3**] recorded in MeCN.	**5**
Fig. S3 ESI-MS spectrum of complex [**2**] recorded in MeCN.	**6**
Fig. S4 ESI-MS spectrum of complex [**1**] recorded in MeCN.	**7**
Fig. S5 ^{1}H NMR spectra of the ligand L_3 in DMSO-d_6.	**8**
Fig. S6 ^{1}H NMR spectra of the complex [**1**] in DMSO-d_6.	**9**
Fig. S7 ^{13}C NMR spectra of the complex [**1**] in DMSO-d_6.	**10**
Fig. S8 ^{1}H-^{1}H COSY NMR spectra of the complex [**1**] in DMSO-d_6.	**11**
Fig. S9 ^{1}H-^{13}C HMBC NMR spectra of the complex [**1**] in DMSO-d_6.	**12**
Fig. S10 ^{1}H-^{13}C HSQC NMR spectra of the complex [**1**] in DMSO-d_6.	**13**
Fig. S11 ^{1}H NMR spectra of the complex [**2**] in DMSO-d_6.	**14**
Fig. S12 ^{1}H-^{1}H COSY NMR spectra of the complex [**2**] in DMSO-d_6.	**15**
Fig. S13 ^{1}H-NMR spectra of the complex [**3**] in DMSO-d_6.	**16**
Fig. S14 ^{13}C-NMR spectra of the complex [**3**] in Acetonitrile-d_3.	**16**
Fig. S15 ^{1}H-^{1}H COSY NMR spectra of the complex [**3**] in acetonitrile-d_3.	**17**
Fig. S16 (a) ^{13}C NMR spectra of **[1]** (25 mM) upon addition of 3.2 equiv. of phosgene (27 mM triphosgene) in CD_3CN containing Et_3N (75 mM). **(b-c)** Partial ^{13}C NMR spectra of **[1]** (25 mM) in the presence of Triphosgene/TEA (27 mM, 75 mM).	**18**
Fig. S17 Stacked ^{13}C NMR spectra of **[1]** (25 mM) upon addition of 1.2 equiv. of DCP in CD_3CN and DCP only.	**19**
Fig. S18 (a) COSY NMR spectra of **[1]-DCP** (25 mM) upon addition of 1.2 equiv. of DCP in CD_3CN. Inset: Partial COSY NMR spectra of **[1]-DCP** (25 mM) in the aliphatic region.	**20**
Fig. S19 Interference experiment of probe **[1]** towards studied CWAs (phosgene and DCP) in the presence of another.	**21**
Fig. S20 (a, b) UV-vis and fluorescence spectra of **[2]** (40 μM) in the presence of triphosgene (0 – 200 μM)/TEA (1 mM) in dry MeCN at 298 K. **(c)** Partial ^{1}H NMR spectra for titration of **[2]** (8 mM) in the presence of triphosgene (10 mM)/TEA (30 mM) in CD_3CN at 298 K. **(d, e)** UV-vis and fluorescence spectra of **[3]** (40 μM) in the presence of triphosgene (0 – 200 μM)/TEA (2 mM) in dry MeCN at 298 K. (λ_{ex} = 450 nm; λ_{em} = 598 nm for **[2]**, **[3]**). **(f)** Partial ^{1}H NMR spectra for titration of **[3]** (8 mM) with triphosgene (10 mM) in the presence of TEA (30 mM) in CD_3CN at 298 K.	**21**

Fig. S21 (a, b) UV-vis and fluorescence spectra of **[2]** (40 μM) in the presence of DCP (0 – 200 μM) in dry MeCN at 298 K (λ_{ex} = 450 nm; λ_{em} = 598 nm for **[2]**). **(c)** Partial ^{1}H NMR spectra for titration of **[2]** with DCP (5 equiv., 2 mM) CD_3CN at 298 K. **(d, e)** UV-vis and fluorescence spectra of **[3]** (40 μM) in the presence of DCP (0 – 200 μM) in dry CH_3CN at 298 K (λ_{ex} = 450 nm; λ_{em} = 598 nm for **[3]**). **(f)** Partial ^{1}H NMR spectra for titration of **[3]** with DCP (5 equiv., 2 mM) CD_3CN at 298 K.	**22**
Fig. S22 UV-vis absorbance spectra of (a) **[1]** and (b) [**2**] (40 μM) in the presence of DECP (0 – 180 μM) in CH_3CN at 298 K.	**23**
Fig. S23 Luminescence titration analysis of **[1]** after addition of nerve agent mimic DECP.	**23**
Fig. S24 Photoluminescence titration analysis of probe **[1]** (30 μM) upon gradual addition of various nerve agent interferents: **(a)** DMEMP, **(b)** TBACl, **(c)** DMTMP, **(d)** $POCl_3$, **(e)** DOPP. **(f)** Ac_2O (acetic anhydride). [λ_{ex} = 433 nm; λ_{em} = 600 nm for (**a-f**)].	**24**
Fig. S25 Photoluminescence titration analysis of probe **[1]** (30 μM) upon gradual addition of various phosgene interferents: **(a)** phosphoryl chloride ($POCl_3$), **(b)** Tetrabutyl ammonium chloride (TBACl), **(e)** acetic anhydride (Ac_2O) **(f)** Chloroacetyl chloride [λ_{ex} = 397 nm; λ_{em} = 597 nm for (**a-d**)].	**25**
Fig. S26 Frontier Molecular Orbitals (FMOs) (LUMOs and HOMOs) for the complex **[1]** computed at the B3LYP functional level of theory using 6-31G** for C, H, N, O, S and SDD basis sets for Ru in acetonitrile.	**25**
Fig. S27 Frontier Molecular Orbitals (FMOs) (LUMOs and HOMOs) for the complex **[1]-phos** computed at the B3LYP functional level of theory using 6-31G** for C, H, N, O, S and SDD basis sets for Ru in acetonitrile.	**26**
Fig. S28 Frontier Molecular Orbitals (FMOs) (LUMOs and HOMOs) for the complex **[1]-DCP** computed at the B3LYP functional level of theory using 6-31G** for C, H, N, O, S and SDD basis sets for Ru in acetonitrile.	**26**
Fig. S29 The plot overlayed with calculated and experimental absorption spectra for the complex **[1]** from TD-DFT.	**27**
Table S1 Key transitions obtained from TD-DFT using B3LYP/SDD/6-31G**level responsible for experimental transitions for **[1]** in CH_3CN.	**27**
Table S2 Optimized atomic coordinates for DFT calculations for Probe **[1]**, [**1]-Phos** and **[1]-DCP.**	**27-36**
Fig. S30 Luminescence changes of an immobilized **[1]-**polystyrene film upon exposure to 20 ppm of Interferents concentrations under 365 nm UV-light.	**37**

Fig. S31 Calculation of the limit of detection (LOD) of phosgene.	**38**
Fig. S32 Calculation of the limit of detection (LOD) of DCP.	**39**

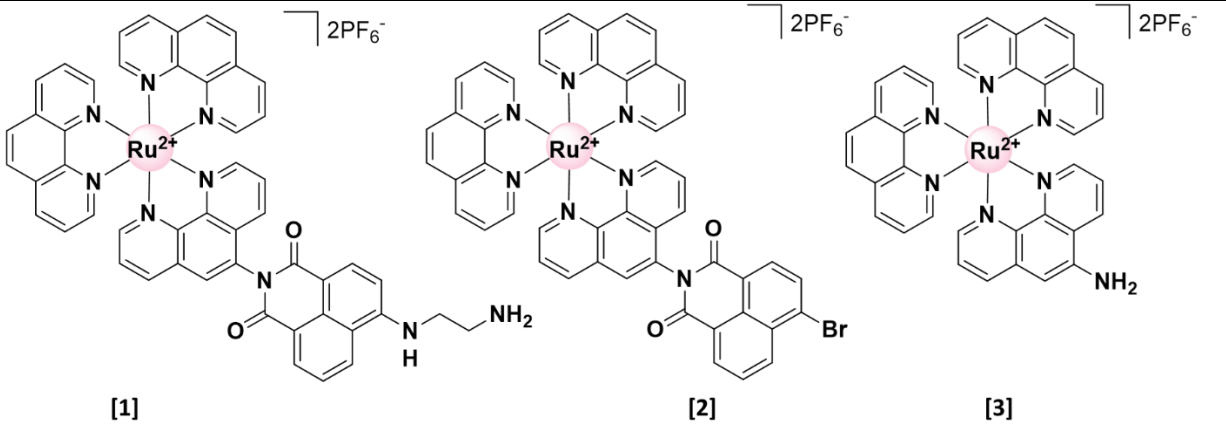

Fig. S1 Structures of ruthenium(II) complexes [**1**]-[**3**] studied in this work. Complex **[1]** was evaluated as the primary luminescent chemodosimetric probe in this study.

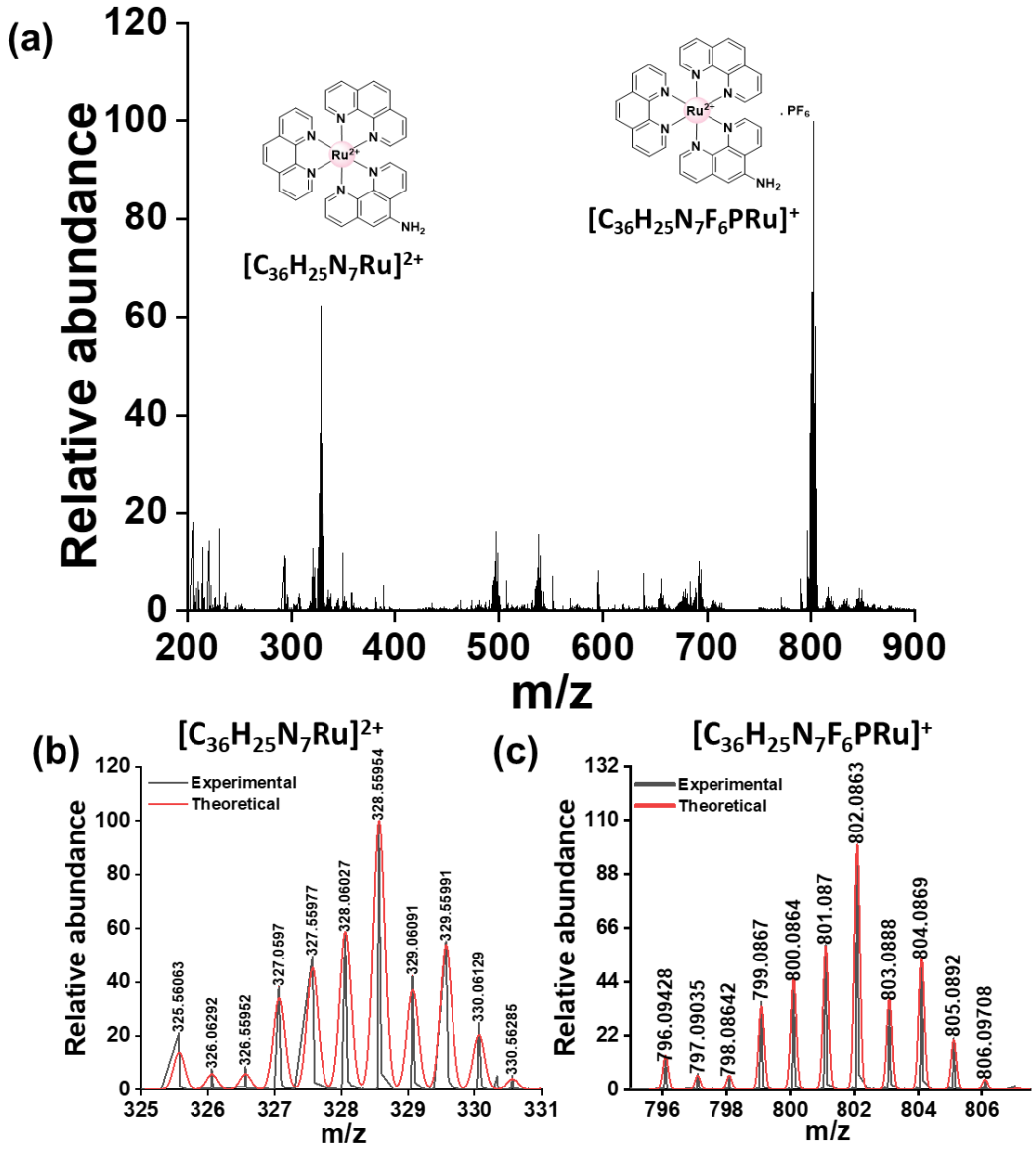

Fig. S2 ESI-MS spectra of complex [**3**] recorded in acetonitrile. The molecular ion peak (M^+) is shown with the experimental and theoretical peak distribution patterns.

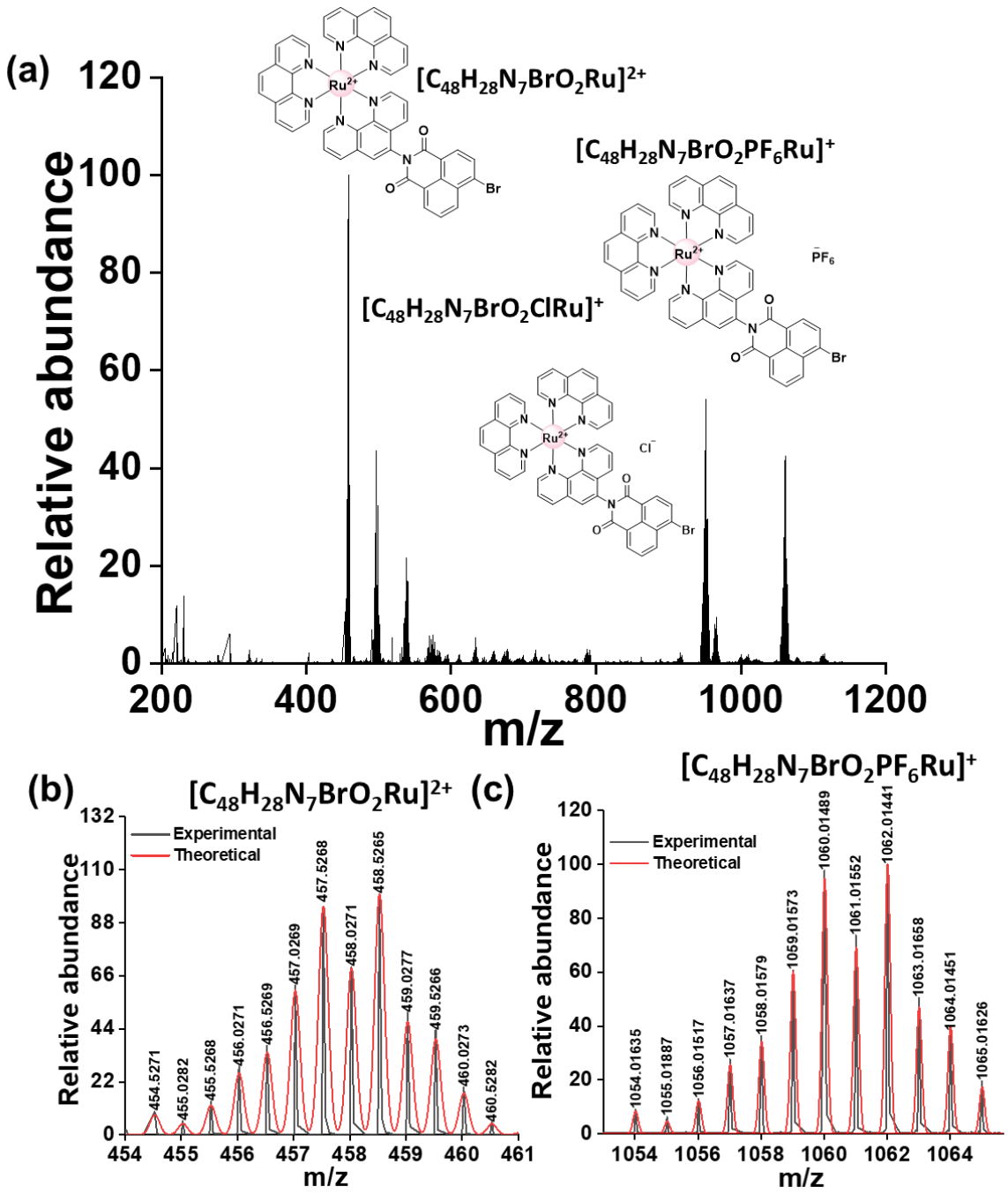

Fig. S3 ESI-MS spectra of complex [**2**] recorded in acetonitrile. The molecular ion peak (M^+) is shown with the experimental and theoretical peak distribution patterns.

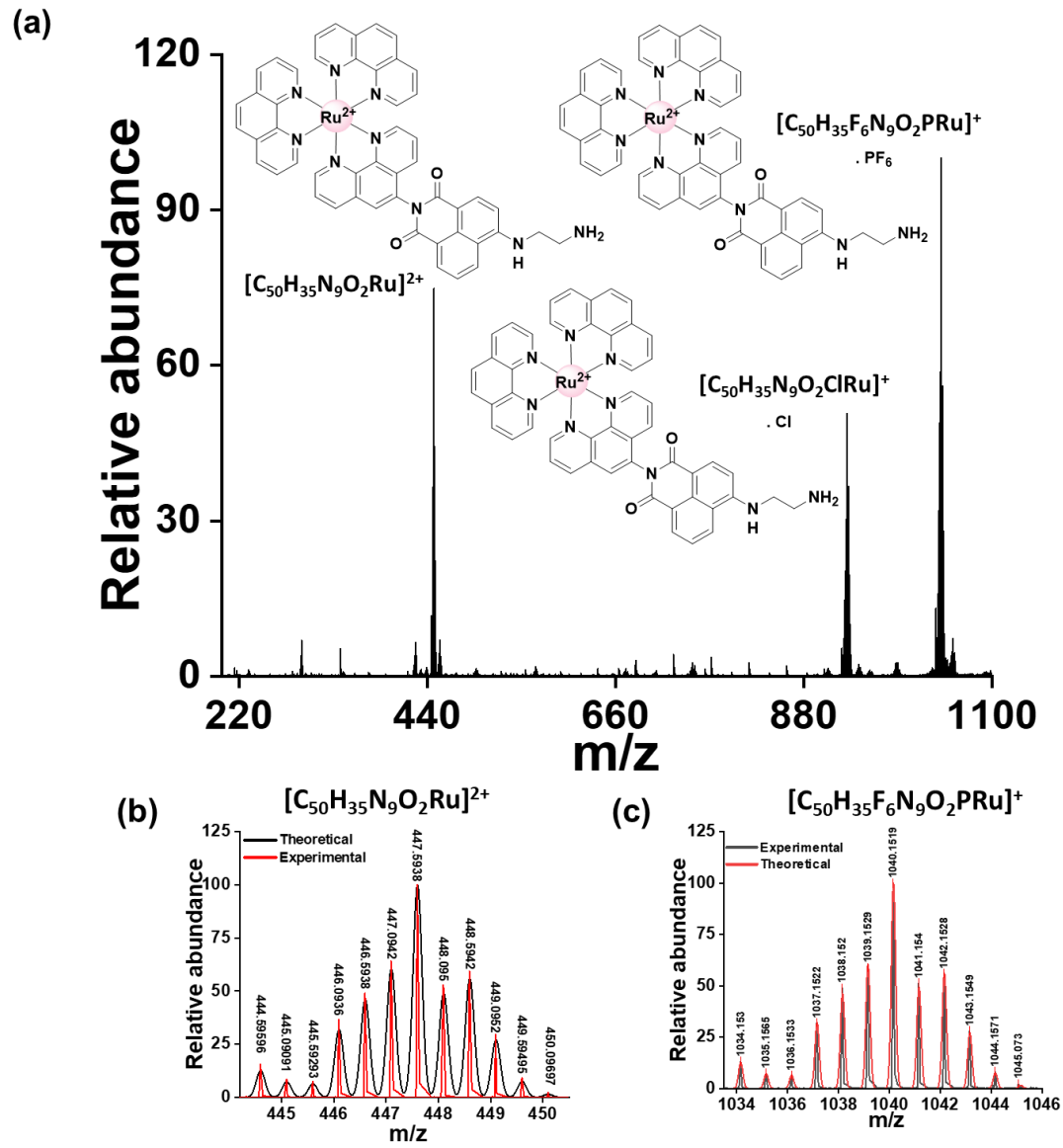

Fig. S4 Full range ESI-MS spectra of complex/probe [**1**] recorded in acetonitrile. Various molecular ion peaks (M^+) speciations are shown in the inset with experimental and theoretical peak distribution patterns.

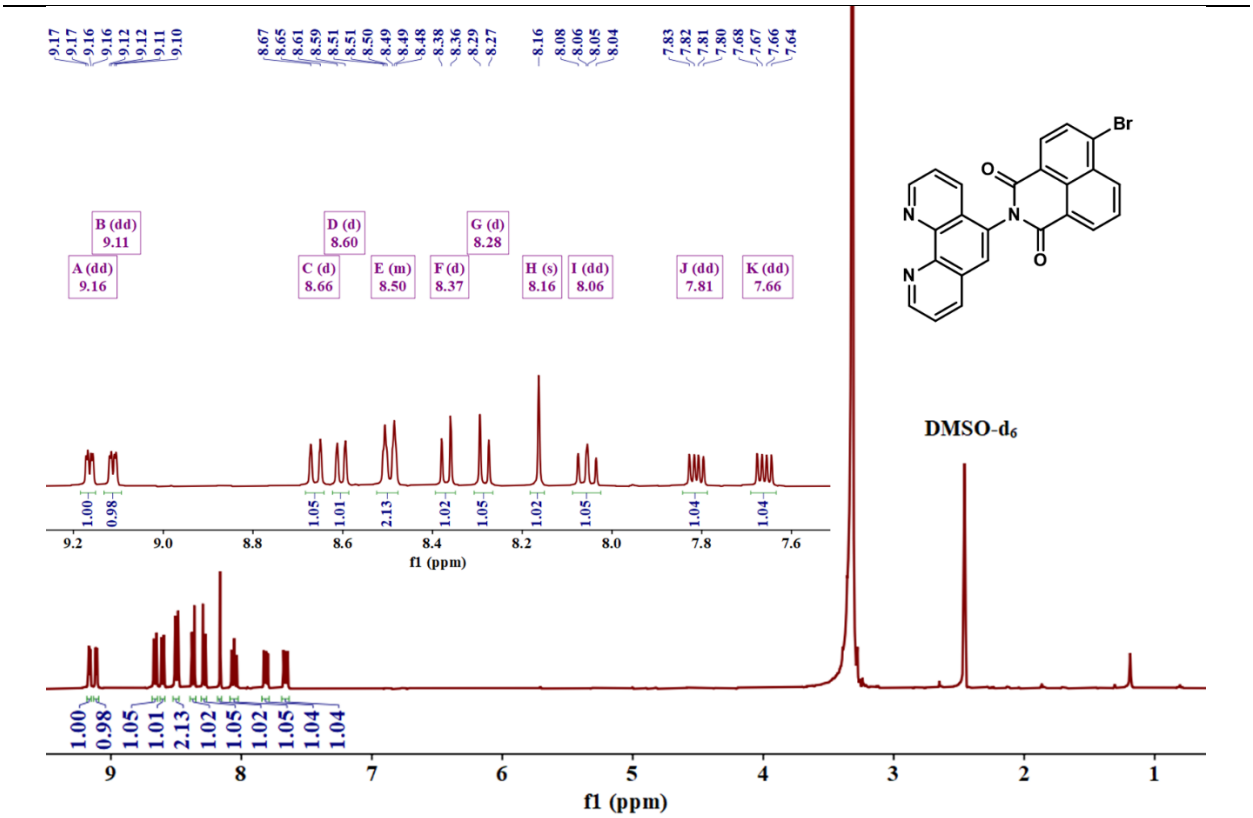

Fig. S5 ^{1}H-NMR spectra of the ligand L_3 in DMSO-d_6 at 298 K. Inset shows the zoom-in ^{1}H-NMR spectra for the aromatic region.

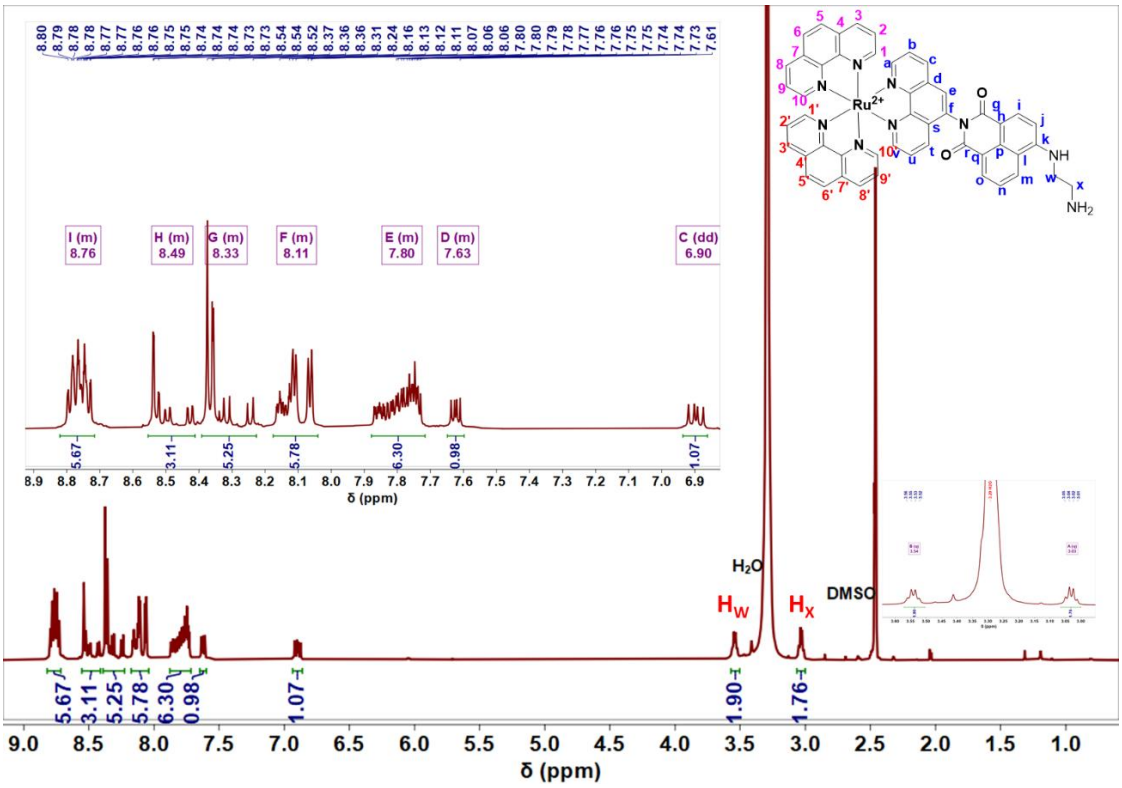

Fig. S6 ^{1}H-NMR spectra of the complex [**1**] in DMSO-d_6 at 298 K. Inset shows the zoom-in ^{1}H NMR spectra for the aromatic region with proposed assignments.

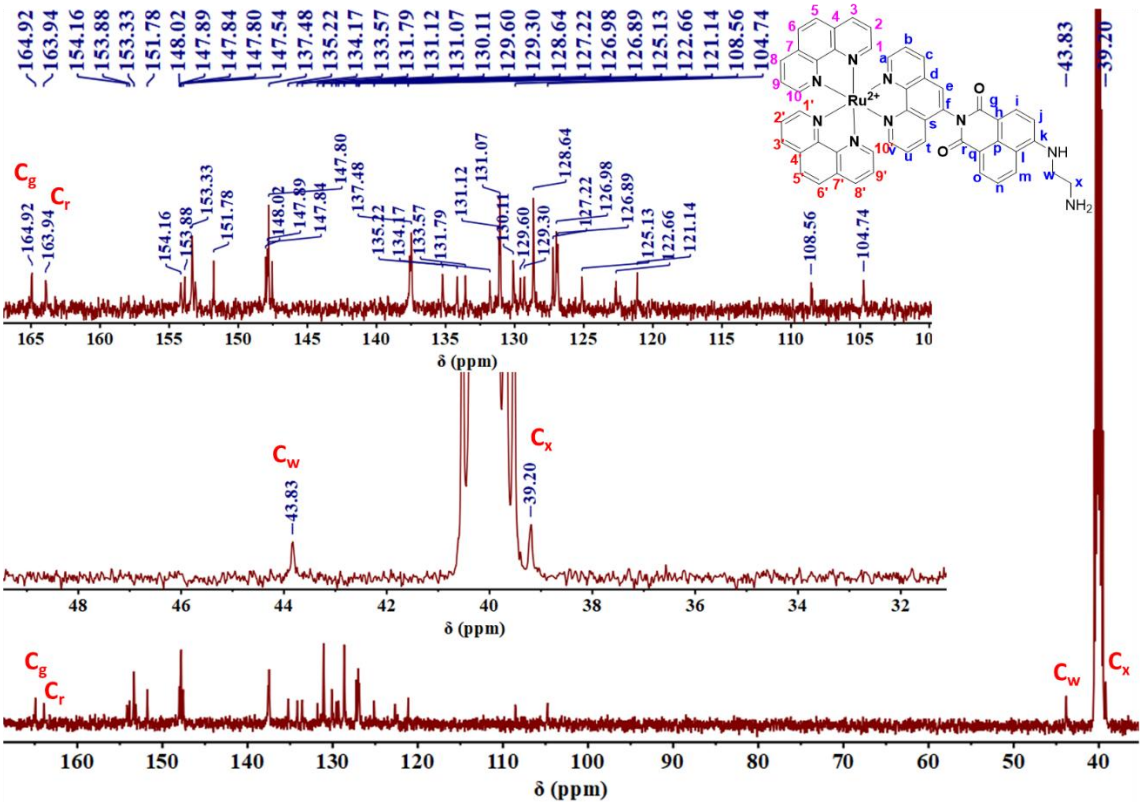

Fig. S7 ^{13}C NMR spectra of the complex [**1**] in DMSO-d_6 at 298 K. Inset shows the zoom-in ^{1}H NMR spectra for the aromatic and aliphatic region.

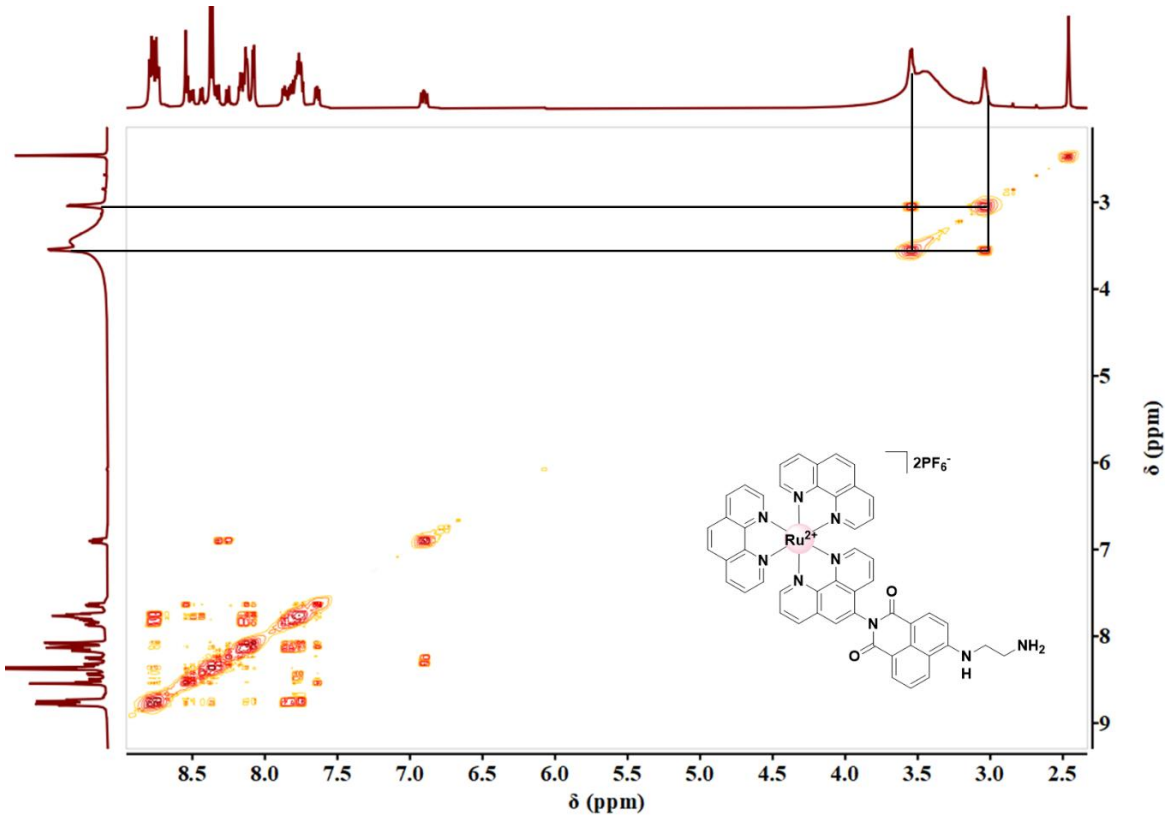

Fig. S8 ^{1}H-^{1}H COSY NMR spectra of the complex [**1**] in DMSO-d_6.

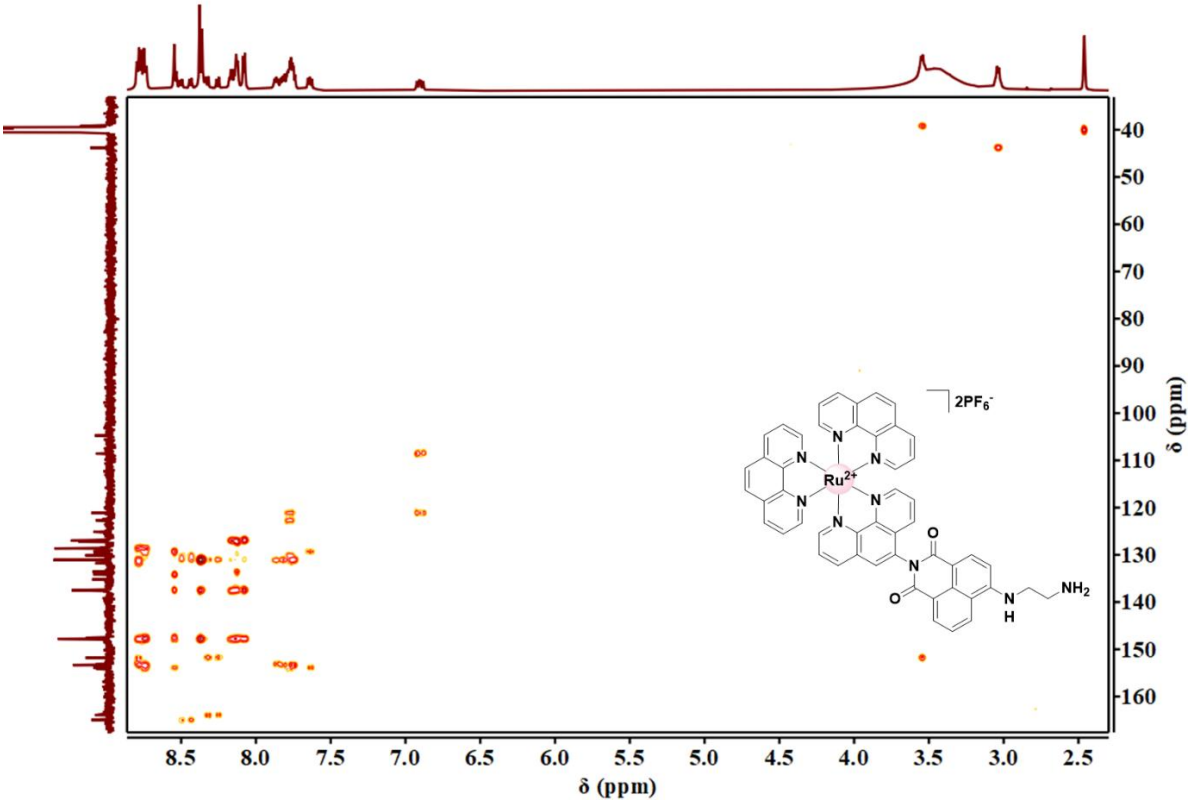

Fig. S9 ^{1}H-^{13}C HMBC NMR spectra of the complex [**1**] in DMSO-d_6.

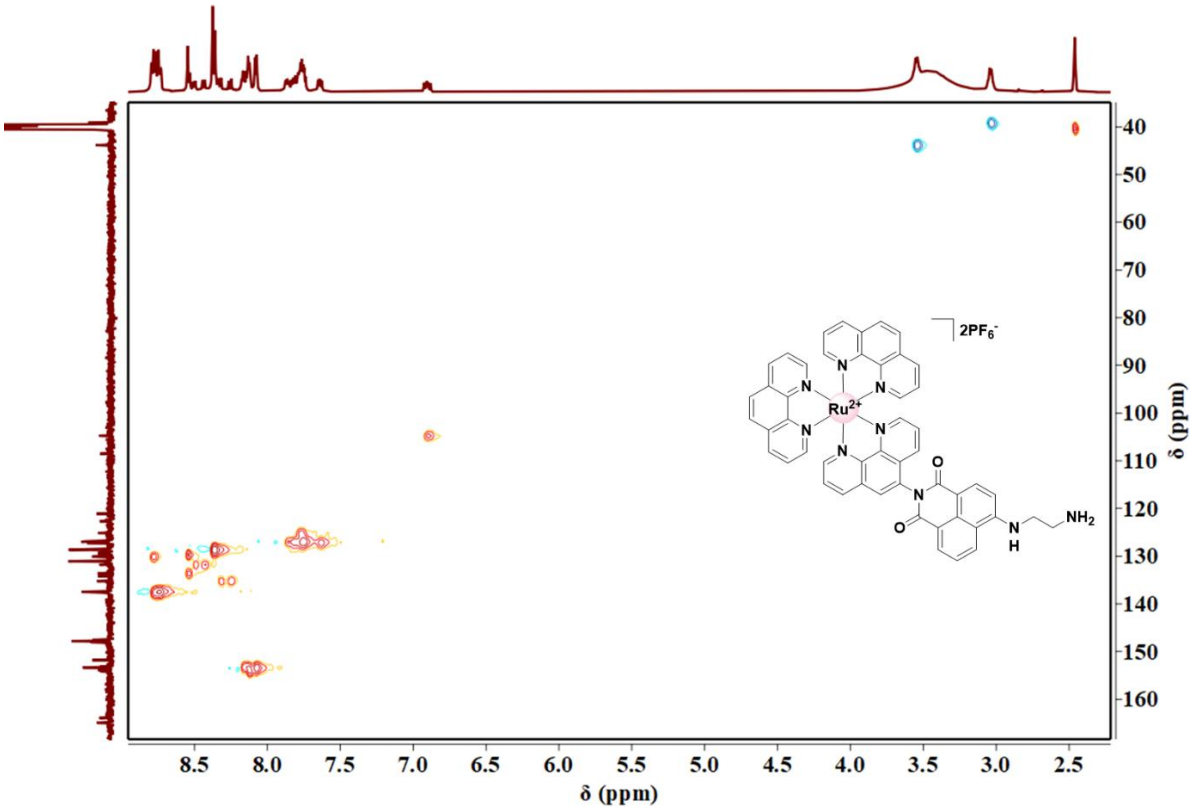

Fig. S10 ^{1}H-^{13}C HSQC NMR spectra of the complex [**1**] in DMSO-d_6.

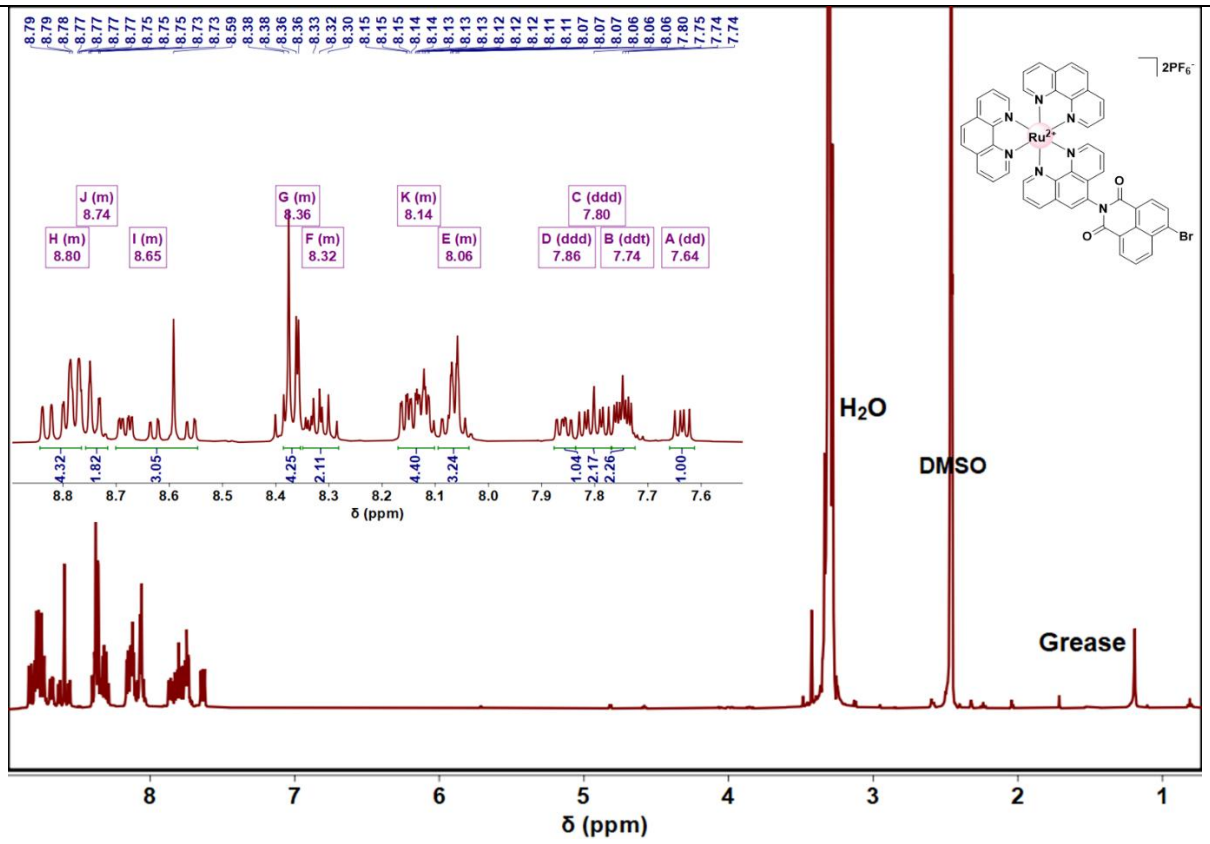

Fig. S11 ^{1}H NMR spectra of the complex [**2**] in DMSO-d_6 at 298 K. Inset shows the zoom-in NMR spectra for the aromatic region.

Fig.

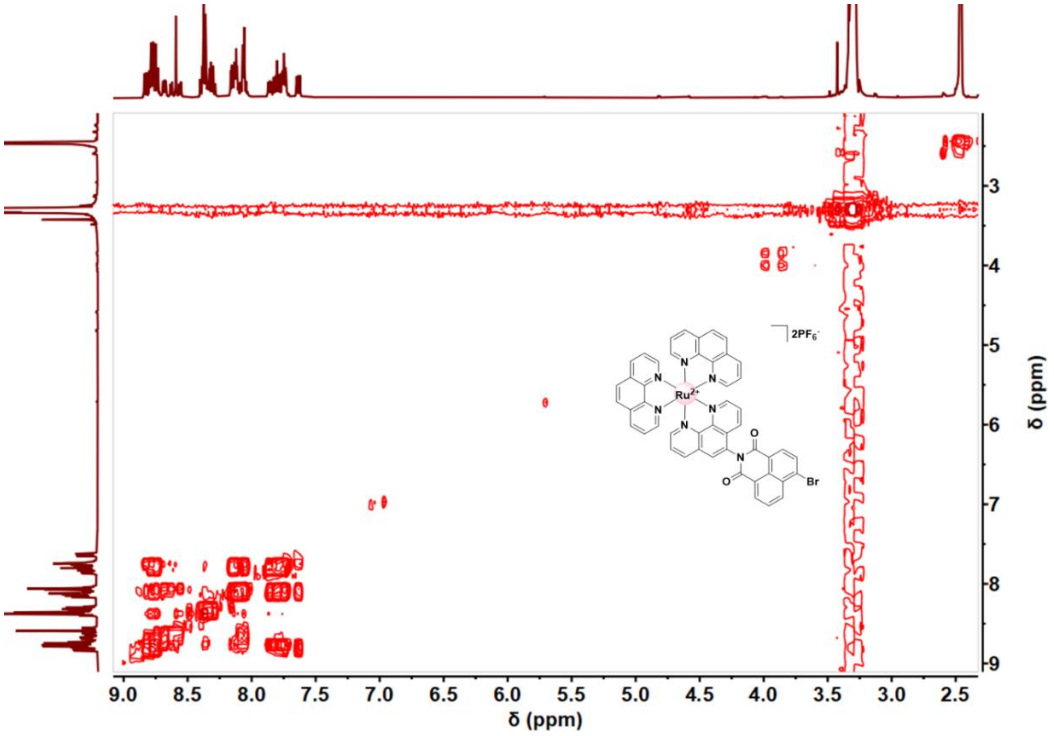

S12 ^{1}H-^{1}H COSY NMR spectra of the complex [**2**] in DMSO-d_6.

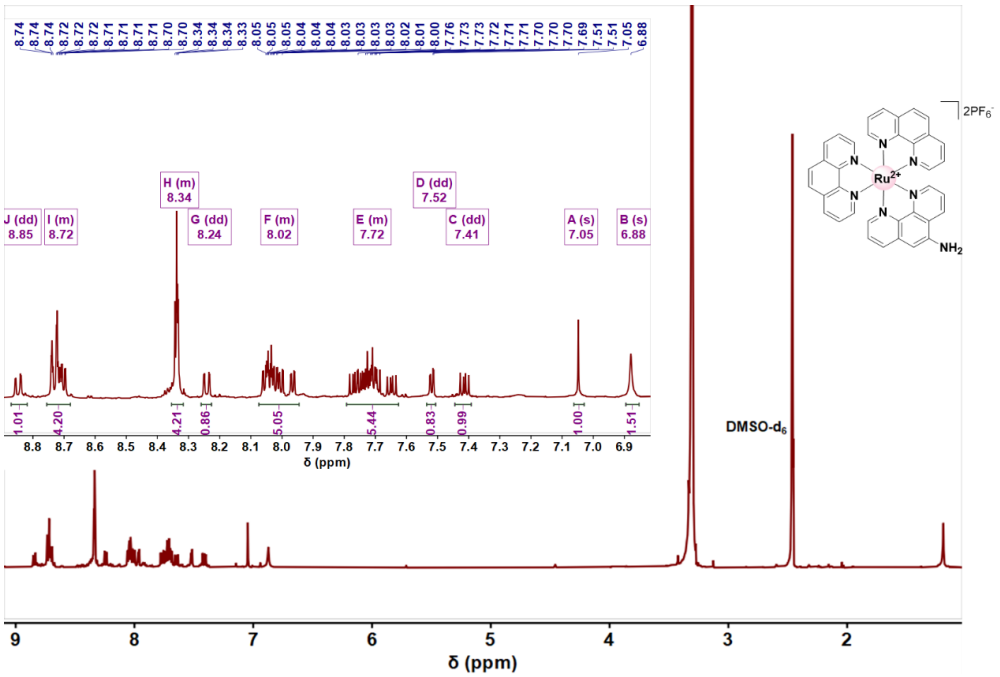

Fig. S13 ^{1}H NMR spectra of the complex [**3**] in DMSO-d_6 at 298 K. Inset shows the zoom-in NMR spectra for the aromatic region.

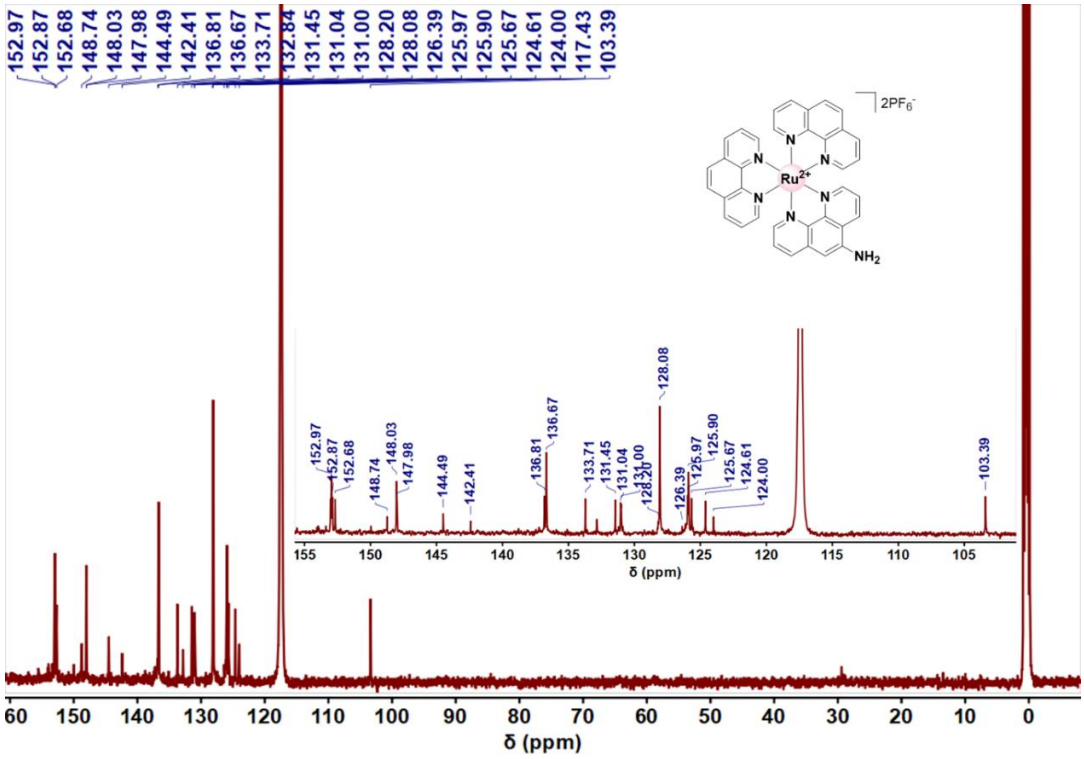

Fig. S14 ^{13}C NMR spectra of the complex [**3**] in acetonitrile-d_3 at 298 K. Inset shows the zoom-in NMR spectra for the aromatic region and aliphatic region.

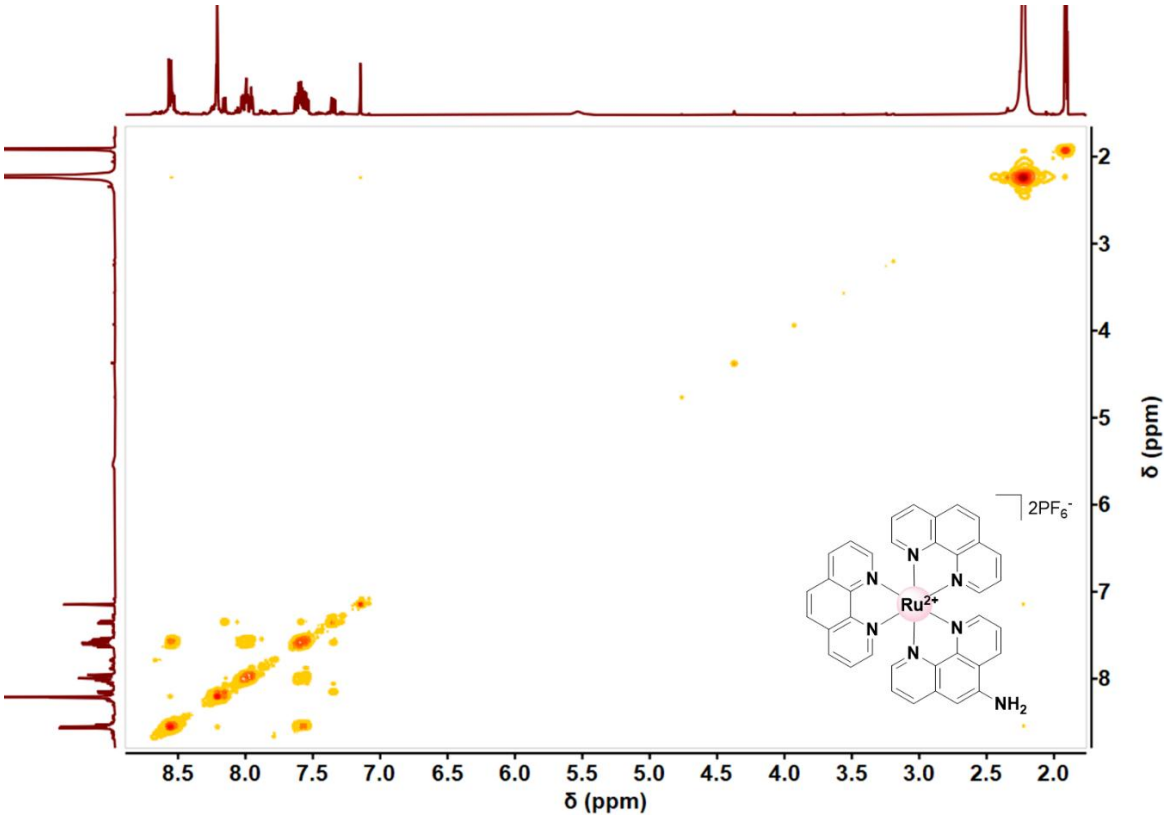

Fig. S15 ^{1}H-^{1}H COSY NMR spectra of the complex [**3**] in acetonitrile-d_3.

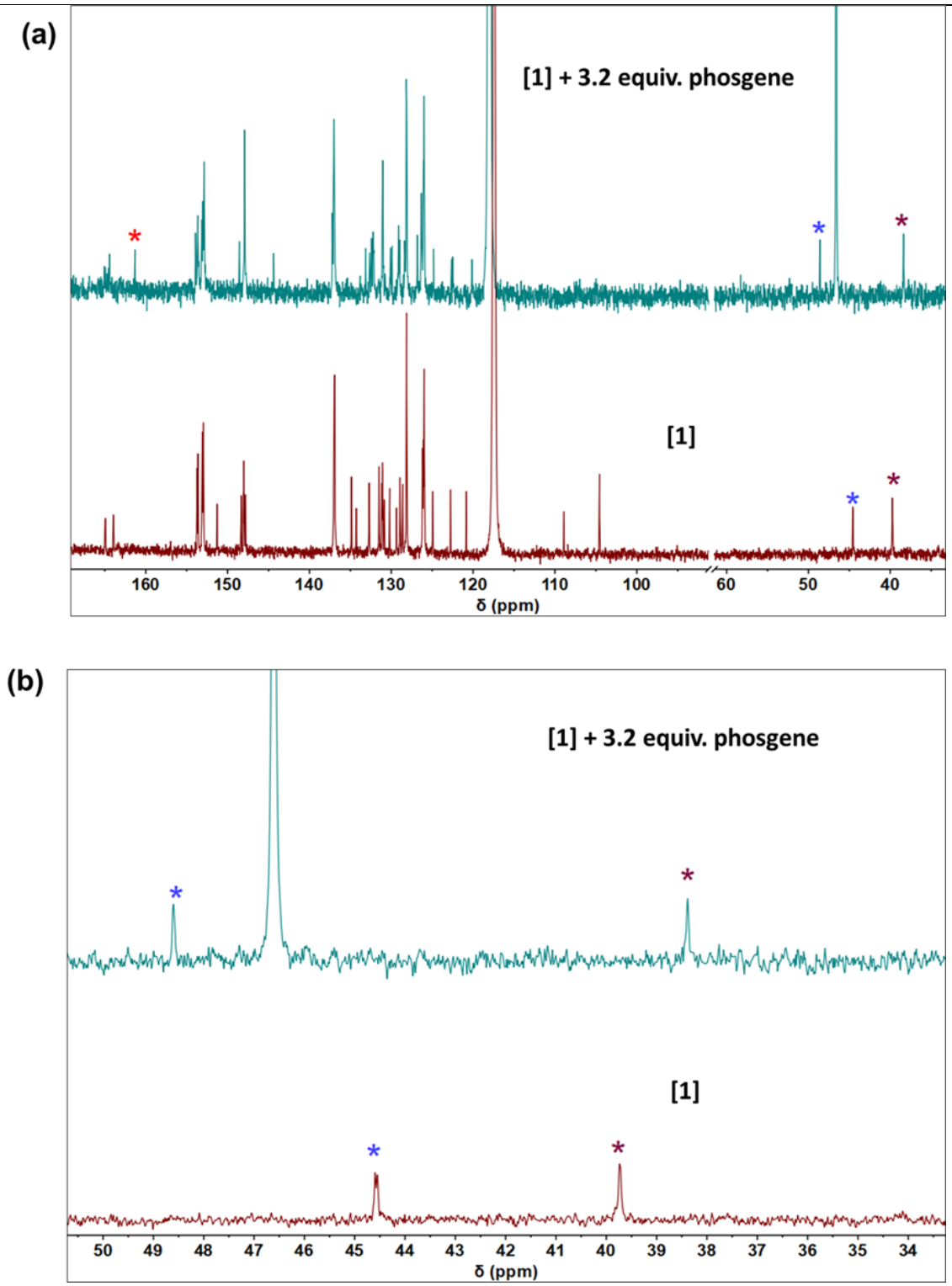

Fig. S16 (a) ^{13}C NMR spectra of **[1]** (25 mM) upon addition of 3.2 equiv. of phosgene (0 – 27 mM triphosgene) in CD_3CN containing Et_3N (75 mM). **(b-c)** Partial ^{13}C NMR spectra of **[1]** (25 mM) in the presence of Triphosgene/TEA (27 mM, 75 mM).

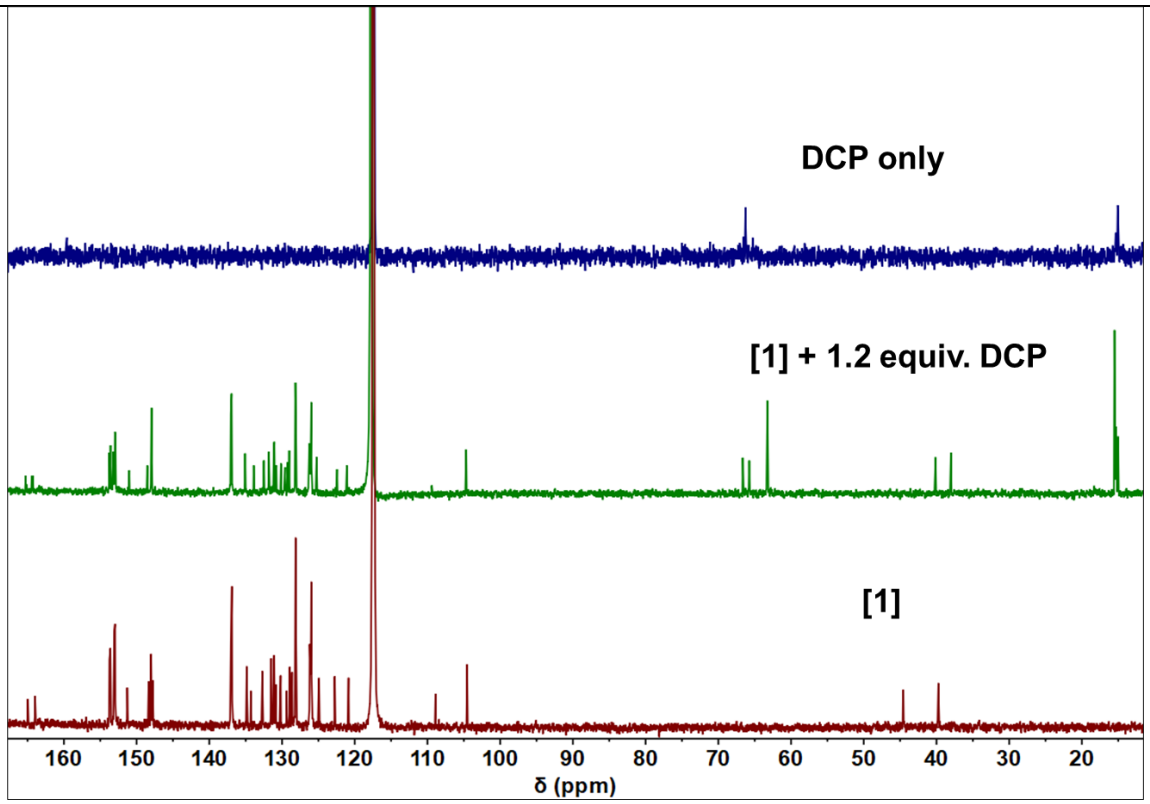

Fig. S17 Stacked ^{13}C NMR spectra of **[1]** (25 mM) upon addition of 1.2 equiv. of DCP in CD_3CN and DCP only.

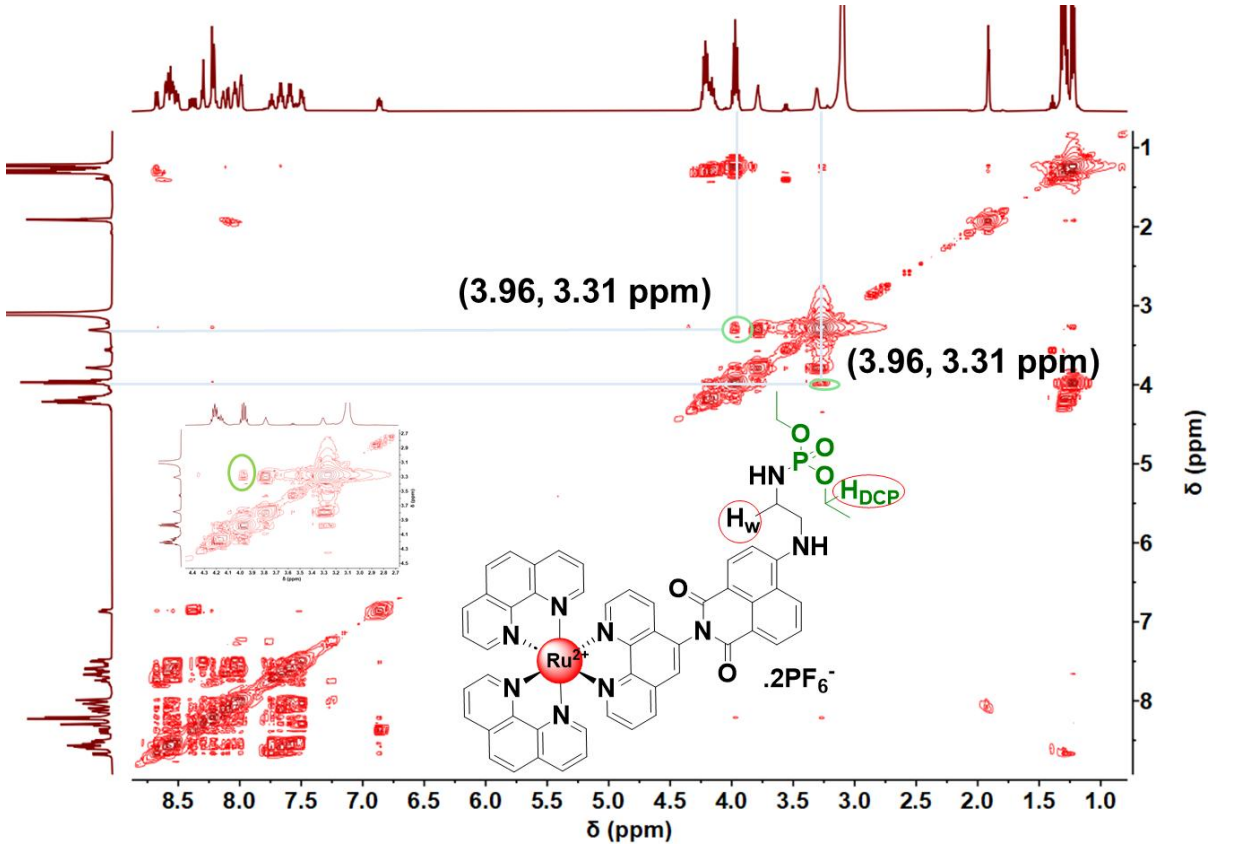

Fig. S18 (a) COSY NMR spectra of **[1]-DCP** (25 mM) upon addition of 1.2 equiv. of DCP in CD_3CN. Inset: Partial COSY NMR spectra of **[1]-DCP** (25 mM) in the aliphatic region.

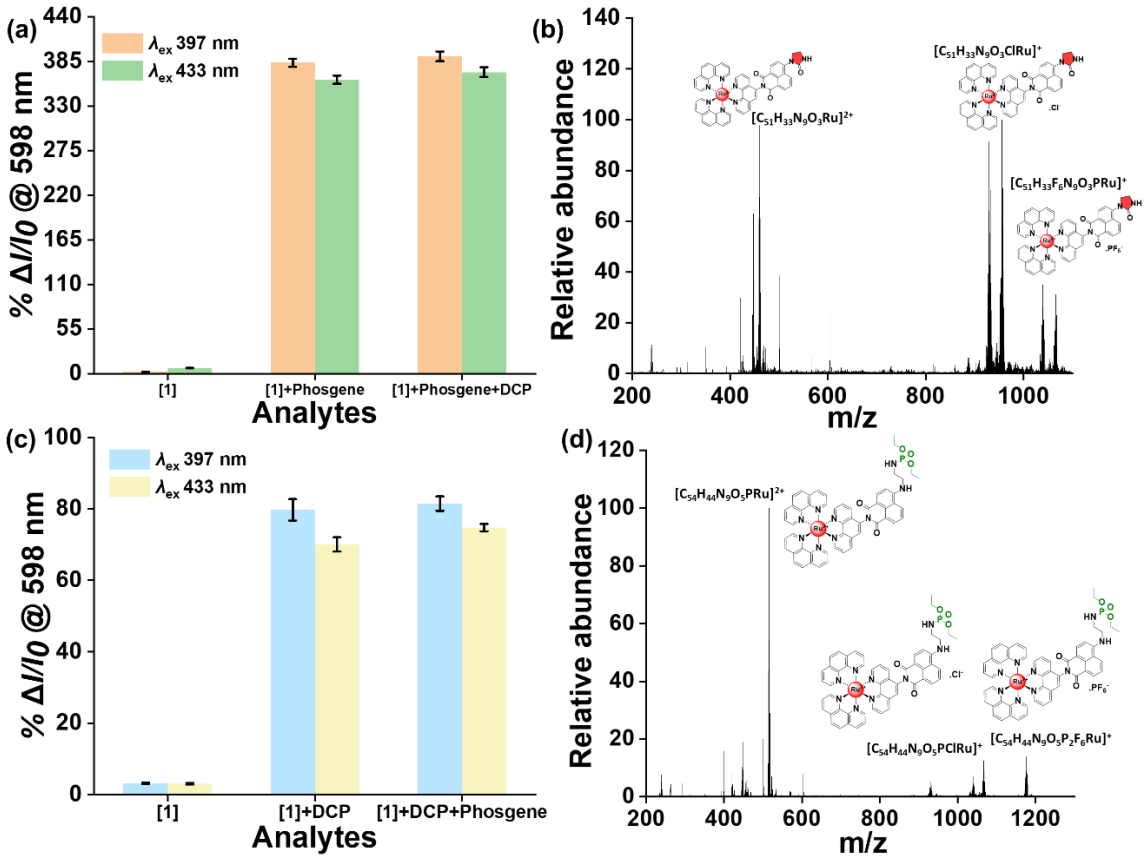

Fig. S19 Interference experiment of probe **[1]** towards studied CWAs (phosgene and DCP) in the presence of another.

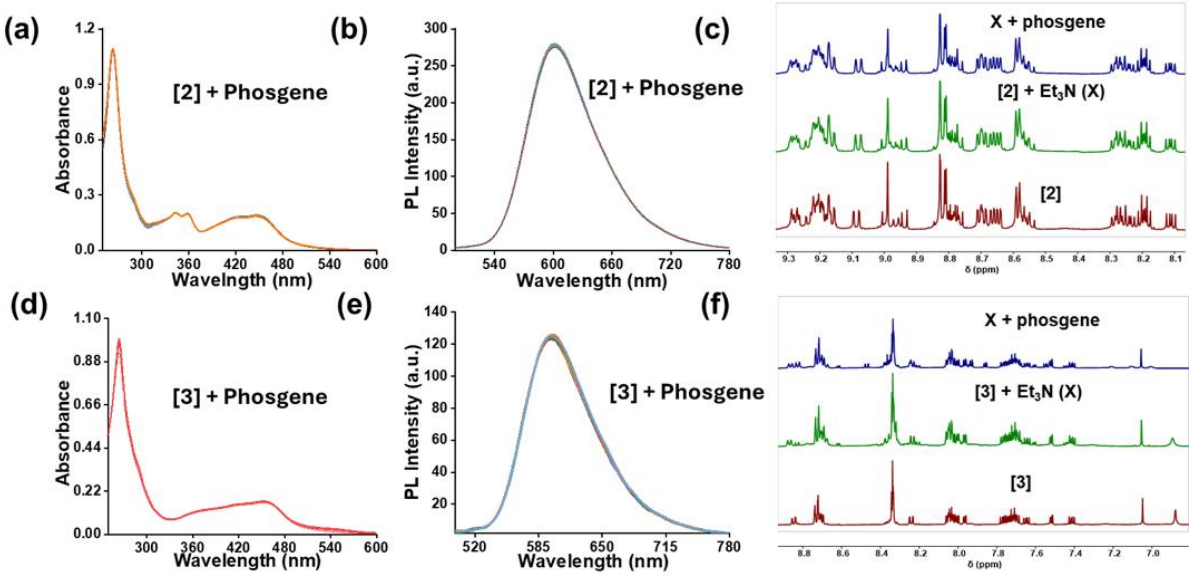

Fig. S20 (a, b) UV-vis and fluorescence spectra of **[2]** (40 μM) in the presence of triphosgene (0 – 200 μM)/TEA (1 mM) in dry MeCN at 298 K. **(c)** Partial ^{1}H NMR spectra for titration of **[2]** (8 mM) in the presence of triphosgene (10 mM)/TEA (30 mM) in CD_3CN at 298 K. **(d, e)** UV-vis and fluorescence spectra of **[3]** (40 μM) in the presence of triphosgene (0 – 200 μM)/TEA (1 mM) in dry MeCN at 298 K. (λ_{ex} = 450 nm; λ_{em} = 598 nm for **[2]**, **[3]**). **(f)** Partial ^{1}H-NMR spectra for titration of **[3]** (8 mM) with triphosgene (10 mM) in the presence of TEA (30 mM) in CD_3CN at 298 K.

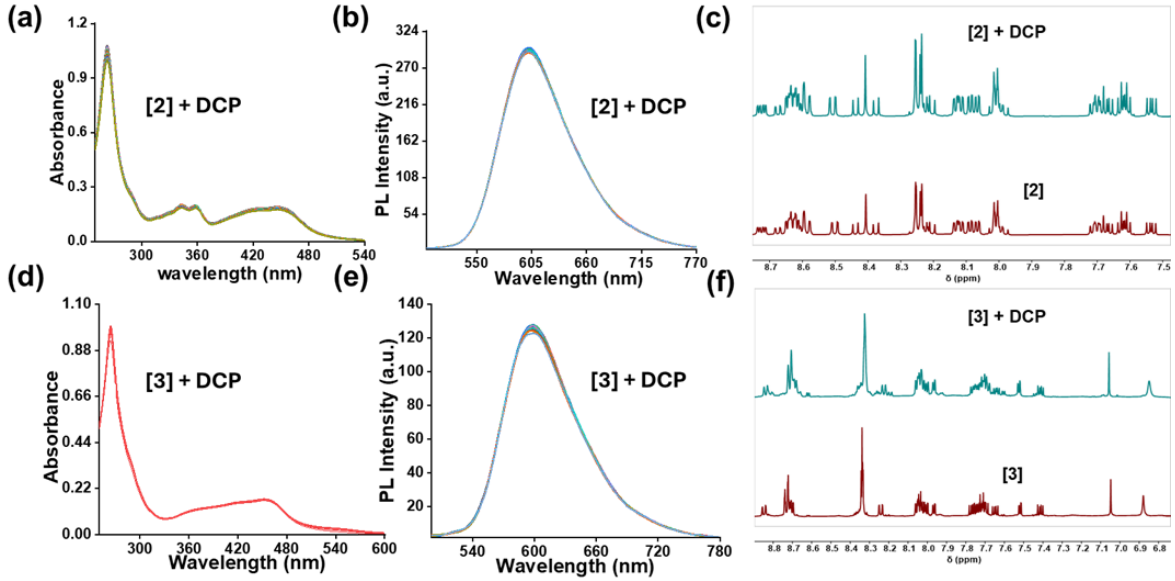

Fig. S21 (a, b) UV-vis and fluorescence spectra of **[2]** (40 μM) in the presence of DCP (0 – 200 μM) in dry MeCN at 298 K (λ_{ex} = 450 nm; λ_{em} = 598 nm for **[2]**). **(c)** Partial ^{1}H NMR spectra for titration of **[2]** with DCP (2 mM) in CD_3CN at 298 K. **(d, e)** UV-vis and fluorescence spectra of **[3]** (40 μM) in the presence of DCP (0 – 200 μM) in dry CH_3CN at 298 K (λ_{ex} = 450 nm; λ_{em} = 598 nm for **[3]**). **(f)** Partial ^{1}H NMR spectra for titration of **[3]** with DCP (2 mM) in CD_3CN at 298 K.

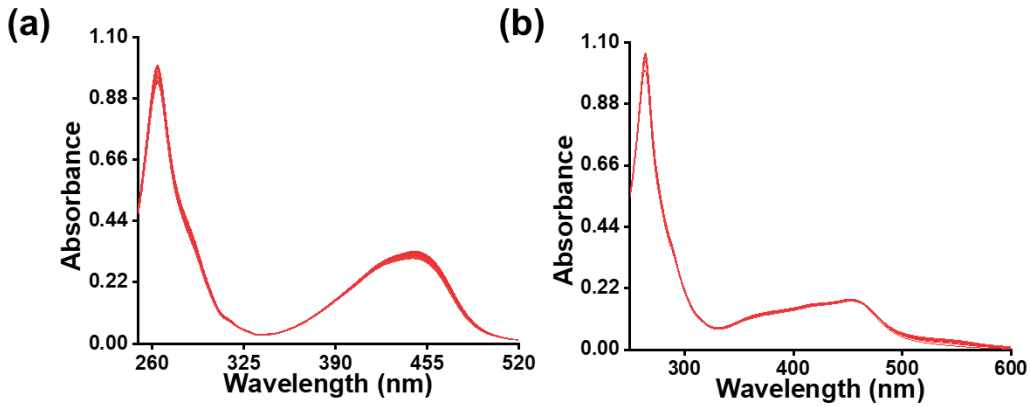

Fig. S22 UV-vis absorbance spectra of [**1**] (a) and [**2**] (b) (40 μM) in the presence of DECP (0 – 180 μM) in CH_3CN at 298 K.

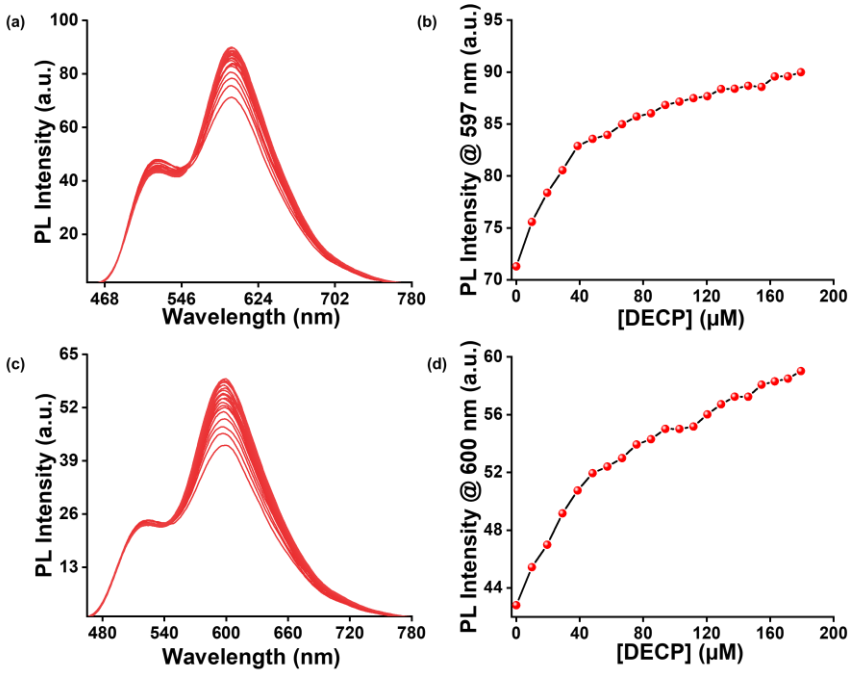

Fig. S23 Photoluminescent analysis of probe [**1**] after addition of DECP. PL titration of [**1**] (30 μM) upon gradual addition of DECP (0 – 180 μM) in MeCN (**a**, **c**), [λ_{ex} = 397 nm; λ_{em} = 597 nm for (**a**)], [λ_{ex} = 433 nm; λ_{em} = 600 nm for (**c**)]. (**b**, **d**) Changes in the emission spectra at 597 nm (**b**), 600 nm (**d**) of Ru-complex [**1**] after the addition of DECP.

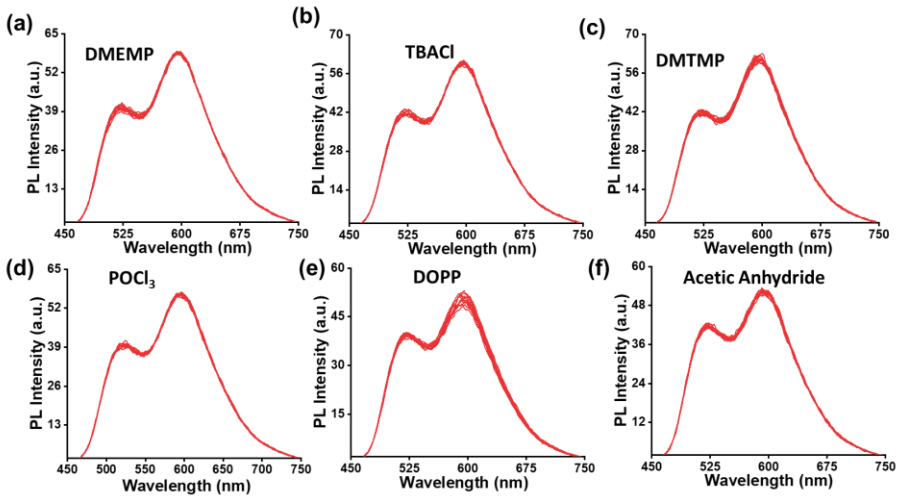

Fig. S24 Photoluminescence titration analysis of probe **[1]** (30 μM) upon gradual addition of various nerve agent interferents: **(a)** diethyl(methoxymethyl)phosphonate (DMEMP), **(b)** tetra-n-butylammonium chloride (TBACl), **(c)** dimethyl trimethylsilylphosphonate (DMTMP), **(d)** phosphoryl chloride ($POCl_3$), **(e)** diethyl-(2-oxopropyl)-phosphonate (DOPP). **(f)** acetic anhydride (Ac_2O). [λ_{ex} = 433 nm; λ_{em} = 600 nm for (**a**-**f**)].

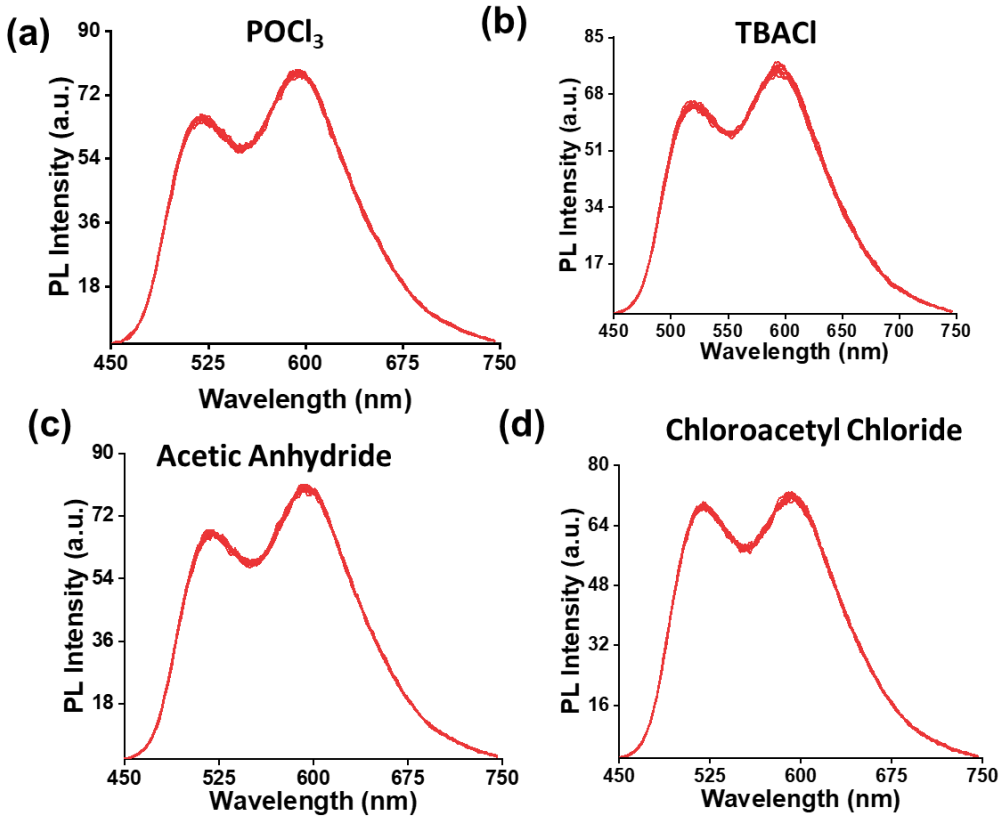

Fig. S25 Photoluminescence titration analysis of probe **[1]** (30 μM) upon gradual addition of various phosgene interferents: **(a)** phosphoryl chloride ($POCl_3$), **(b)** Tetrabutyl ammonium chloride (TBACl), **(c)** acetic anhydride (Ac_2O) **(d)** Chloroacetyl chloride [λ_{ex} = 397 nm; λ_{em} = 597 nm for (**a-d**)].

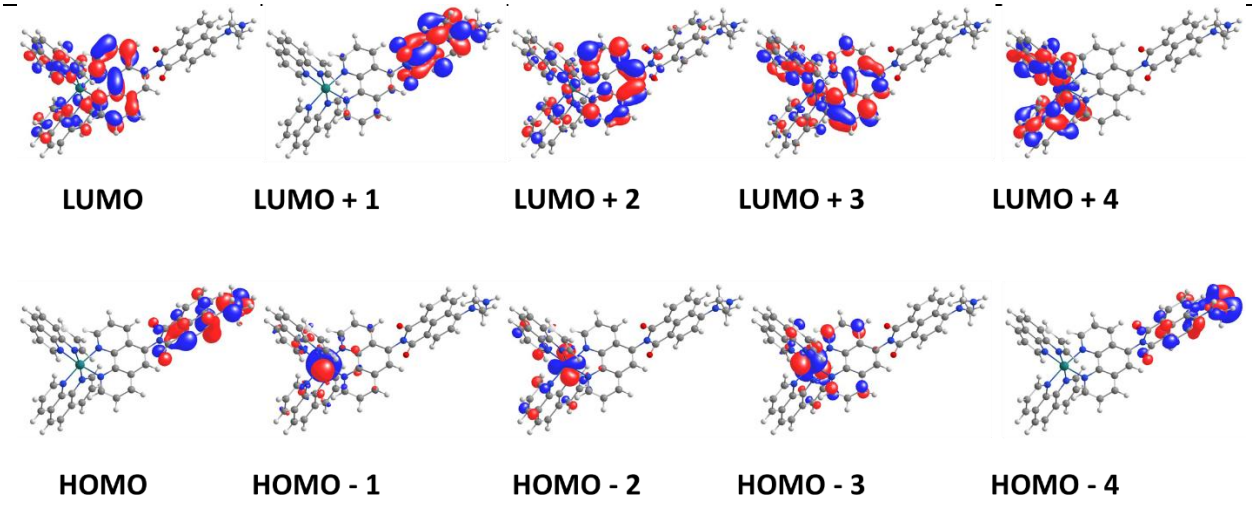

Fig. S26 FMOs (LUMOs and HOMOs) for the complex **[1]** computed at the B3LYP functional level of theory using 6-31G** for C, H, N, O, S, and SDD basis sets for Ru in acetonitrile.

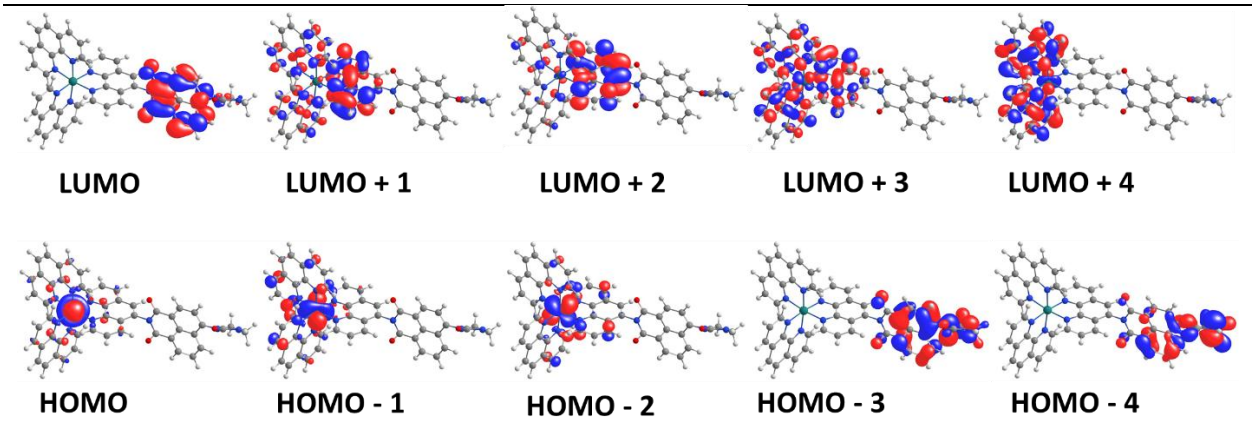

Fig. S27 FMOs (LUMOs and HOMOs) for the complex **[1]phos** computed at the B3LYP functional level of theory using 6-31G** for C, H, N, O, S, and SDD basis sets for Ru in acetonitrile.

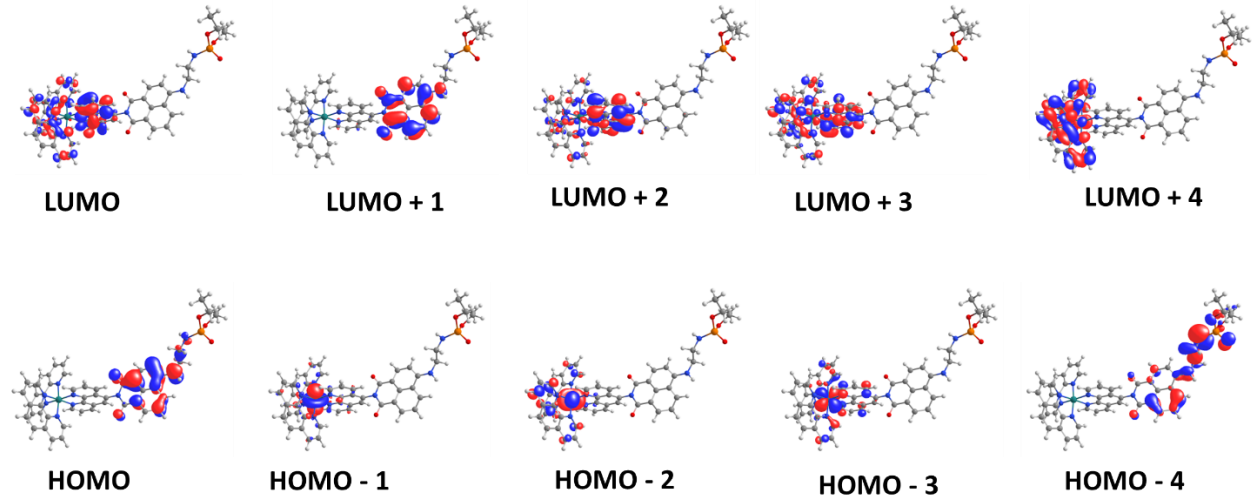

Fig. S28 FMOs (LUMOs and HOMOs) for the complex **[1]DCP** computed at the B3LYP functional level of theory using 6-31G** for C, H, N, O, S, and SDD basis sets for Ru in acetonitrile.

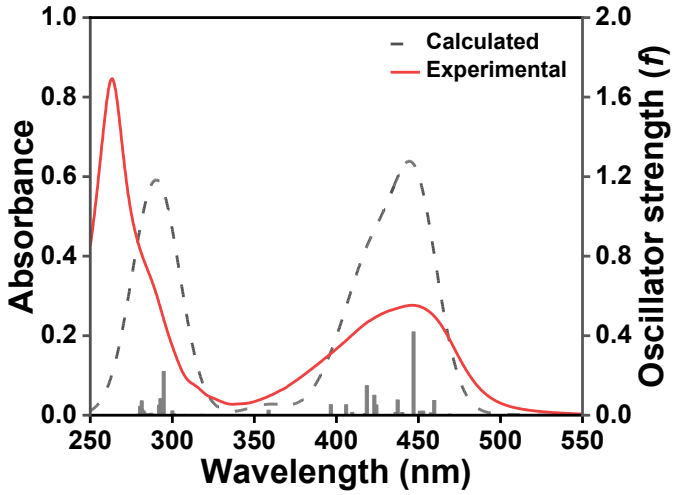

Fig. S29 The plot overlayed with calculated and experimental absorption spectra for the complex **[1]** from TD-DFT.

Table S1. Key transitions obtained from TD-DFT) using B3LYP/SDD/6-31G**level responsible for experimental transitions for **[1]** in CH_3CN.

Complexes	λ_{cal} (eV/nm)	λ_{exp} (eV/nm)	Oscillator strength (f)	Key transitions	Contribution
[1]	2.78 / 447	2.71 / 447	0.4192	HOMO-3→LUMO+2 HOMO-3→LUMO+3 HOMO-2→LUMO+4 HOMO→LUMO HOMO→LUMO+1 HOMO→LUMO+2	3% 4% 7% 4% 77% 4%

Table S2. Optimized atomic coordinates for DFT calculations for Probe **[1]**, **[1]phos** and **[1]DCP**

Atomic coordinates for all calculated species **[1]**			
C	0.6048	0.8929	1.8391
H	1.3737	1.0983	2.5722
C	-0.7574	1.1338	2.1322
H	-1.0203	1.534	3.1045
C	-1.736	0.8545	1.1794
C	-1.3418	0.3318	-0.0822
C	-2.2625	-0.0016	-1.1493

C	-1.818	-0.5062	-2.3454
H	-2.5283	-0.7501	-3.1294
C	-0.4129	-0.7211	-2.5847
C	0.1054	-1.2364	-3.8043
C	1.4842	-1.4032	-3.9354
H	1.9189	-1.7927	-4.8487
C	2.3421	-1.0608	-2.8638
H	3.4139	-1.1808	-2.9544
C	0.0441	0.1205	-0.3056
C	0.5102	-0.4029	-1.5546
C	1.9544	-2.6899	1.3116
H	1.0714	-2.1244	1.58
C	2.0707	-4.0562	1.6605
H	1.2573	-4.5295	2.1986
C	3.219	-4.768	1.3125
H	3.3265	-5.8163	1.5739
C	4.2587	-4.1021	0.6056
C	4.0663	-2.7306	0.2881
C	5.0759	-2.0055	-0.4234
C	6.2801	-2.6501	-0.8142
C	7.2444	-1.8766	-1.5184
H	8.1781	-2.3316	-1.8345
C	6.9704	-0.5366	-1.7935
H	7.6805	0.0845	-2.3274
C	5.7451	0.0335	-1.3743
H	5.5164	1.0701	-1.5863
C	4.2242	0.0294	2.864
H	3.9646	-1.0206	2.9064
C	4.8761	0.6572	3.9516
H	5.1159	0.0671	4.8287
C	5.1969	2.0133	3.8819
H	5.695	2.5113	4.7082
C	4.8609	2.7448	2.7089
C	4.2099	2.0434	1.6586

C	3.8439	2.7245	0.4531
C	4.1254	4.1085	0.2983
C	3.7357	4.7291	-0.921
H	3.932	5.7852	-1.0786
C	3.1035	3.9631	-1.9008
H	2.7913	4.4008	-2.8421
C	2.8612	2.5876	-1.674
H	2.3776	1.9804	-2.4283
N	1.0068	0.3937	0.6504
N	1.8763	-0.5688	-1.6945
N	2.9261	-2.0311	0.6431
N	4.8103	-0.6769	-0.7061
N	3.8917	0.6989	1.7387
N	3.2217	1.9711	-0.5272
Ru	2.9538	-0.0333	0.0161
C	5.1425	4.1513	2.5337
C	4.7878	4.8068	1.3761
H	5.641	4.6836	3.3386
H	5.0016	5.8646	1.2528
C	5.4884	-4.7427	0.1991
C	6.4603	-4.0448	-0.4818
H	7.3823	-4.5337	-0.7831
H	5.6309	-5.7914	0.4438
H	-0.5678	-1.4926	-4.6163
H	-2.7838	1.0314	1.3957
C	-4.2251	1.4594	-1.3014
C	-4.4314	-0.8821	-0.3827
C	-5.6789	1.6367	-1.1113
C	-5.8612	-0.6674	-0.2117
C	-6.4699	0.5743	-0.5727
N	-3.6834	0.2048	-0.9372
C	-6.2645	2.8577	-1.4656
H	-5.6383	3.646	-1.8708
C	-7.8827	0.7721	-0.3975

C	-6.6654	-1.6917	0.3216
C	-8.0408	-1.5288	0.507
H	-8.6118	-2.347	0.9278
C	-8.69	-0.3149	0.1569
O	-3.4665	2.3577	-1.7611
O	-3.8177	-1.9454	-0.0764
N	-10.0397	-0.1609	0.3201
H	-10.4607	0.7265	0.078
C	-10.9565	-1.1656	0.8848
H	-11.9645	-0.9319	0.5236
H	-10.7009	-2.1625	0.5053
C	-10.9699	-1.1808	2.4434
H	-9.9578	-1.3805	2.8159
H	-11.256	-0.1849	2.8033
N	-11.8893	-2.1765	3.0205
H	-12.8706	-2.0012	2.8102
H	-11.6361	-3.1413	2.8124
C	-8.4424	2.0258	-0.7713
C	-7.652	3.0523	-1.2957
H	-8.1063	3.9983	-1.5716
H	-9.5044	2.2207	-0.6578
H	-6.1955	-2.6313	0.5966

Atomic coordinates for all calculated species **[1]Phos**			
C	0.9426	1.0074	1.8144
H	1.7286	1.2812	2.506
C	-0.4144	1.2521	2.127
H	-0.6567	1.7253	3.0714
C	-1.4147	0.884	1.2284
C	-1.0475	0.2679	0.0013
C	-1.9897	-0.1631	-1.0105
C	-1.5709	-0.7484	-2.1786
H	-2.2981	-1.0632	-2.9208

C	-0.1691	-0.9544	-2.4435
C	0.3245	-1.5465	-3.6381
C	1.7022	-1.6976	-3.7975
H	2.1188	-2.144	-4.693
C	2.5826	-1.2634	-2.7789
H	3.6537	-1.3703	-2.8916
C	0.3352	0.0608	-0.2461
C	0.7757	-0.546	-1.4664
C	2.3587	-2.5875	1.5159
H	1.474	-2.0199	1.774
C	2.5157	-3.9223	1.9584
H	1.7312	-4.3701	2.5576
C	3.6665	-4.636	1.6223
H	3.8046	-5.6603	1.9548
C	4.6675	-4.0039	0.8333
C	4.4356	-2.6631	0.4248
C	5.4051	-1.9724	-0.3714
C	6.6093	-2.6205	-0.7568
C	7.5324	-1.8818	-1.5482
H	8.4646	-2.3403	-1.864
C	7.2201	-0.5708	-1.9091
H	7.8981	0.0234	-2.5111
C	5.9976	0.0048	-1.4891
H	5.7396	1.0187	-1.7667
C	4.6167	0.282	2.7878
H	4.3819	-0.7668	2.9161
C	5.2907	1.001	3.8032
H	5.5729	0.4818	4.712
C	5.5786	2.3543	3.6237
H	6.0932	2.9217	4.393
C	5.1868	2.991	2.4133
C	4.5172	2.2014	1.4402
C	4.0962	2.7847	0.2016
C	4.3401	4.1591	-0.0627

C	3.896	4.6803	-1.3097
H	4.0618	5.7259	-1.5506
C	3.2507	3.8313	-2.2093
H	2.8979	4.1921	-3.1688
C	3.0483	2.4713	-1.8754
H	2.555	1.8	-2.5665
N	1.3195	0.4219	0.6572
N	2.1402	-0.6962	-1.6348
N	3.293	-1.9614	0.7676
N	5.1015	-0.6731	-0.7391
N	4.2321	0.8603	1.629
N	3.4605	1.9486	-0.6997
Ru	3.2559	-0.0152	-0.0033
C	5.4301	4.3863	2.1269
C	5.0217	4.9478	0.938
H	5.943	4.9863	2.8731
H	5.207	5.9979	0.7315
C	5.8966	-4.6488	0.4314
C	6.8302	-3.9836	-0.331
H	7.7522	-4.4754	-0.6273
H	6.0698	-5.674	0.7457
H	-0.366	-1.8722	-4.4096
H	-2.458	1.0653	1.4616
C	-3.9997	1.2297	-1.2604
C	-4.1056	-0.9945	-0.0777
C	-5.4525	1.3929	-1.0433
C	-5.5541	-0.8013	0.1131
C	-6.2014	0.3696	-0.3843
N	-3.4103	0.0324	-0.7739
C	-6.0808	2.5631	-1.4763
H	-5.4918	3.3281	-1.9722
C	-7.6146	0.5415	-0.1949
C	-6.2966	-1.7718	0.7916
C	-7.6921	-1.6294	0.9555

H	-8.2561	-2.4068	1.4572
C	-8.3607	-0.5078	0.4535
O	-3.28	2.0846	-1.8383
O	-3.4701	-1.9993	0.3358
C	-8.2177	1.7652	-0.6183
C	-7.4666	2.7548	-1.2478
H	-7.939	3.6813	-1.5574
H	-9.2696	1.9352	-0.4166
H	-5.7921	-2.6549	1.1706
C	-10.6828	-0.4688	-0.6201
C	-12.0904	-0.3661	0.0256
H	-10.5461	-1.4283	-1.1346
H	-10.4961	0.3386	-1.3292
H	-12.4756	0.6606	-0.0054
H	-12.8089	-1.029	-0.4628
C	-10.4833	-0.7274	1.7437
O	-9.9799	-0.9088	2.8863
N	-11.817	-0.7862	1.4122
H	-12.5302	-0.8597	2.1253
N	-9.7735	-0.4053	0.5664

Atomic coordinates for all calculated species **[1]DCP**

C	-2.41472000	-0.30591900	1.90154300
H	-3.07210700	-0.12657100	2.74229800
C	-1.05383400	-0.63260800	2.10333400
H	-0.67823500	-0.70591200	3.11735800
C	-0.21915000	-0.85207300	1.00852200
C	-0.75785500	-0.74562800	-0.30257200
C	0.00596400	-0.94654000	-1.51651400
C	-0.57464200	-0.82870500	-2.75426900
H	0.01947600	-0.98303900	-3.64979200
C	-1.97104900	-0.50009500	-2.89177000
C	-2.62536000	-0.36693600	-4.14700100
C	-3.98292900	-0.04665000	-4.17009600
H	-4.51845900	0.06423700	-5.10590200

C	-4.68565700	0.13824000	-2.95630300
H	-5.74037400	0.38104000	-2.95987800
C	-2.13390700	-0.41834700	-0.42646400
C	-2.74175800	-0.29643700	-1.71761000
C	-3.50858600	3.03381700	0.29045400
H	-2.64845200	2.47847600	0.64178600
C	-3.44845200	4.43962200	0.14124700
H	-2.52364800	4.95174100	0.38115300
C	-4.56851900	5.14048700	-0.30673700
H	-4.54077700	6.21943000	-0.42501500
C	-5.75887700	4.42268300	-0.60969300
C	-5.74013400	3.01253600	-0.43710100
C	-6.90705000	2.23376800	-0.72569900
C	-8.09402000	2.86483400	-1.18563500
C	-9.21855700	2.03698500	-1.45775600
H	-10.14485200	2.47950000	-1.81119200
C	-9.11014400	0.65940700	-1.26541400
H	-9.94524800	-0.00317400	-1.46202900
C	-7.89193300	0.10457200	-0.80685700
H	-7.79196300	-0.96287000	-0.65824500
C	-5.75051000	1.34987900	2.95339600
H	-5.40697300	2.30738700	2.58390700
C	-6.27447700	1.22589000	4.26191500
H	-6.33087000	2.10866700	4.88846000
C	-6.70478500	-0.01817900	4.72409200
H	-7.10691400	-0.13211300	5.72609900
C	-6.61057700	-1.14710600	3.86347000
C	-6.07790100	-0.94132200	2.56250800
C	-5.95965900	-2.03764400	1.64847100
C	-6.36824400	-3.34175400	2.03693100
C	-6.22480600	-4.38922600	1.08499100
H	-6.52520100	-5.40051900	1.34190800
C	-5.69761700	-4.09588800	-0.17302200
H	-5.57270800	-4.86742700	-0.92417100

C	-5.31654500	-2.76977300	-0.48680700
H	-4.91087000	-2.52681700	-1.46049900
N	-2.95177500	-0.19534700	0.66746800
N	-4.08884700	0.01546300	-1.75008300
N	-4.62574900	2.32639500	0.01323900
N	-6.80732700	0.86549000	-0.54250700
N	-5.64717000	0.29550600	2.11507700
N	-5.44359300	-1.75501300	0.39586200
Ru	-4.92709600	0.25887600	0.14941000
C	-7.02304800	-2.47939100	4.24171200
C	-6.90473200	-3.53409800	3.36478500
H	-7.42904700	-2.63241800	5.23756800
H	-7.21560900	-4.53280000	3.65759600
C	-6.97418600	5.04827400	-1.07845100
C	-8.09650200	4.30003800	-1.35403200
H	-9.00614600	4.77842500	-1.70561500
H	-6.98413100	6.12649600	-1.20926100
H	-2.07035200	-0.51431800	-5.06811100
H	0.82673600	-1.09979600	1.15258400
C	1.77202800	-2.64468900	-1.38897400
C	2.34260400	-0.18691400	-1.36316700
C	3.21524400	-2.95569400	-1.33525400
C	3.75613900	-0.53585800	-1.31195800
C	4.17956100	-1.90072100	-1.30115600
N	1.41600800	-1.27570900	-1.41346800
C	3.61871600	-4.29554500	-1.32116300
H	2.86369100	-5.07471500	-1.34678200
C	5.57780000	-2.23003000	-1.25524800
C	4.72725700	0.48040600	-1.27226900
C	6.09460200	0.19162000	-1.22608100
H	6.79939600	1.01302500	-1.19056700
C	6.56128400	-1.14862300	-1.22225400
O	0.86933400	-3.52617100	-1.41262400
O	1.89014300	0.99415000	-1.36574600

N	7.90140300	-1.43312700	-1.19861600
H	8.19505500	-2.40065300	-1.17418500
C	8.98705700	-0.44290600	-1.18282000
H	9.88304000	-0.91787300	-1.59494500
H	8.73926100	0.40172400	-1.83519800
C	9.30390700	0.06770000	0.24771400
H	8.40673800	0.50014900	0.70518600
H	9.61690800	-0.77696900	0.87010500
N	10.37285200	1.07980400	0.22591000
H	10.13616000	2.01398700	-0.09042300
C	5.94978600	-3.60393600	-1.24495400
C	4.99172500	-4.62060700	-1.27621800
H	5.30430400	-5.65961300	-1.26668200
H	6.99341900	-3.90146300	-1.21238500
H	4.39779600	1.51516000	-1.27625300
P	11.94676100	0.79251600	0.76772700
O	12.39090000	-0.73069300	0.73557400
O	12.78856900	1.88578000	-0.22346700
O	12.08729700	1.47807200	2.32877500
C	12.91714800	0.85535500	3.40100000
H	12.70115600	-0.21797900	3.43405700
H	13.97549700	1.00106600	3.15453200
C	14.16285200	2.35877500	0.11413300
H	14.12552600	2.86563200	1.08517600
H	14.82872400	1.48976600	0.17842200
C	12.54337000	1.55315700	4.70335000
H	11.48179400	1.40705900	4.93210900
H	13.13729300	1.13421300	5.52607900
H	12.74696400	2.62812800	4.64284100
C	14.58317000	3.30616600	-1.00217700
H	15.59357400	3.68378300	-0.79954300
H	14.59370400	2.78958900	-1.96826500
H	13.90005500	4.16049300	-1.06495600

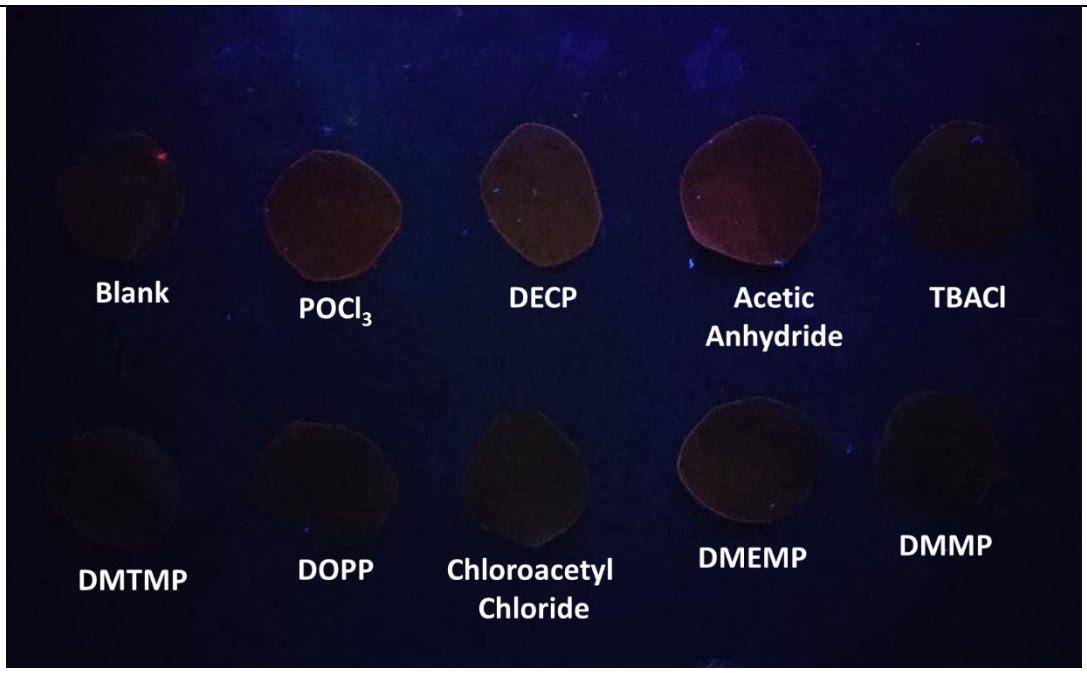

Fig. S30 Luminescence changes of an immobilized **[1]-**polystyrene film upon exposure to 20 ppm of Interferents concentrations under 365 nm UV-light.

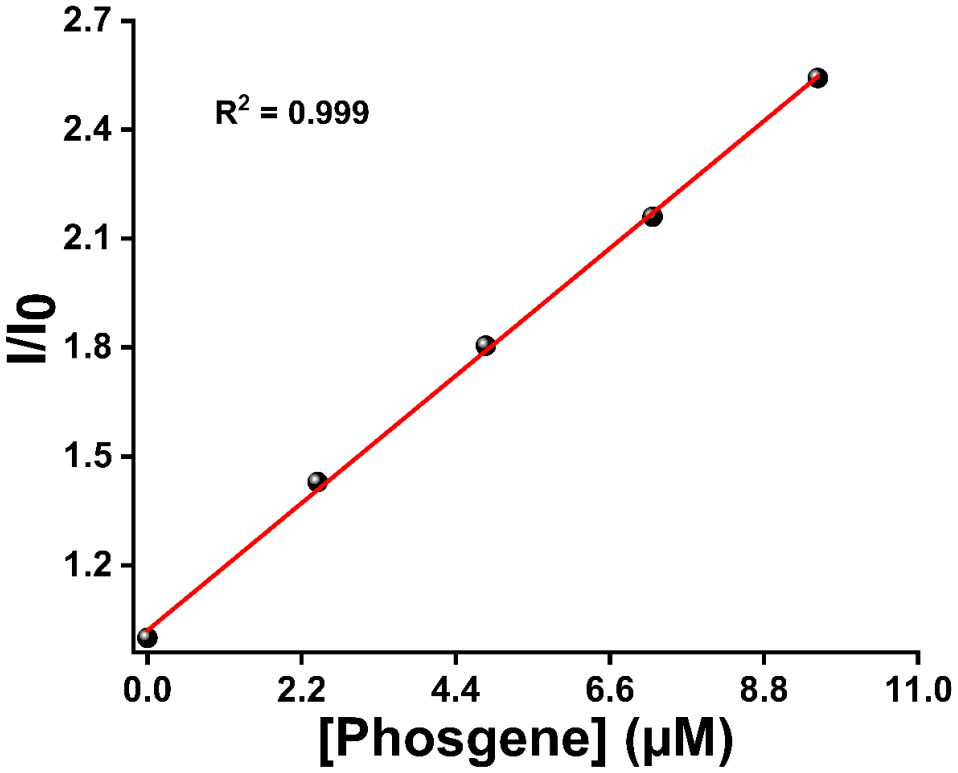

Fig. S31 Calculation of the limit of detection (LOD) of phosgene measured from the relative changes in the luminescence intensity (I/I_0) at 598 nm upon increased concentration of phosgene to **[1]** (30 μM) in acetonitrile at λ_{ex} = 397 nm, T= 298 K.

Limit of Detection Calculations:

LOD = $3.3\sigma/s$

Where, σ is the standard deviation of the regression line and s is the slope of the curve.

For **[1]** vs. phosgene titration: s = 0.1595 and σ = 0.6036.

LOD = **126 nM.**

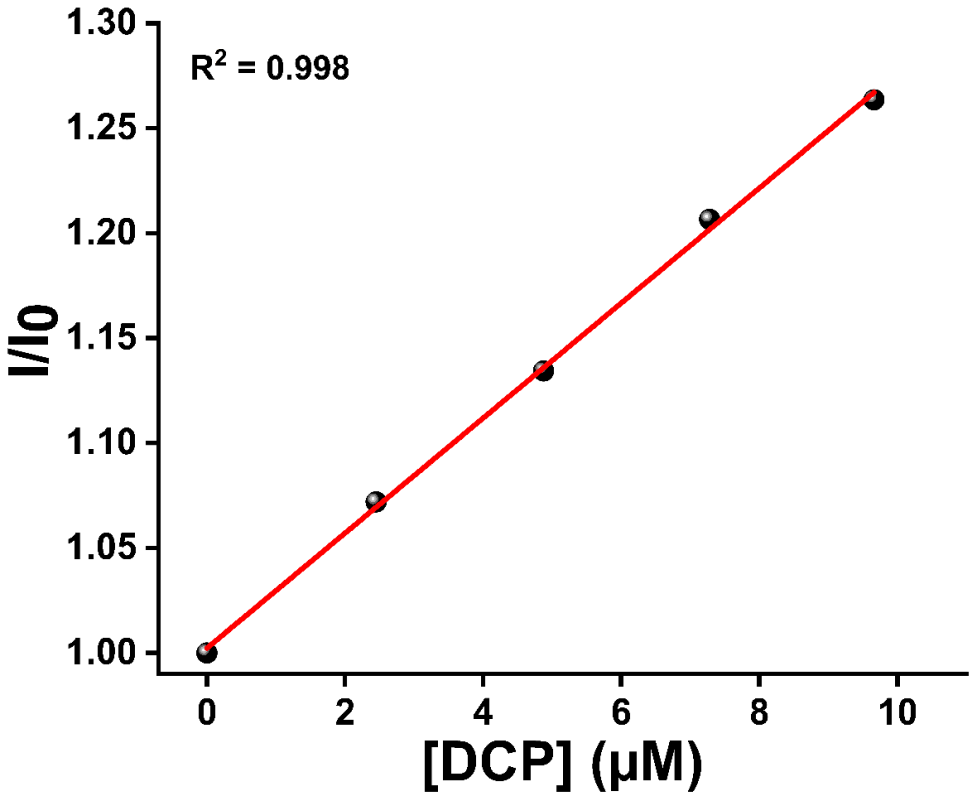

Fig. S32 Calculation of the limit of detection (LOD) of DCP measured from the relative changes in the luminescence intensity (I/I_0) at 597 nm upon increased concentration of DCP to **[1]** (30 μM) in acetonitrile at λ_{ex} = 433 nm, T= 298 K.

Limit of Detection Calculations:

LOD = $3.3\sigma/s$

Where, σ is the standard deviation of the regression line and s is the slope of the curve.

For **[1]** vs. DCP titration: s = 0.0274 and σ = 0.10469.

LOD = **73 nM.**

Luminescence quantum yield calculation

Emission quantum yields for the Ruthenium complexes **[1]**, **[2]** and **[3]** were calculated relative to the reference complex $[Ru(bpy)_3](PF_6)_2$ (λ_{ex} = 450 nm, MeCN, Φ = 0.062 %) in acetonitrile using the equation (1).[1, 2]

$$\Phi_S = \Phi_R\left(\frac{I_S}{I_R}\right)\left(\frac{A_R}{A_S}\right)\left(\frac{\eta_S}{\eta_R}\right)^2$$

Where, Φ_S, Φ_R are the luminescence quantum yield of the sample and the reference respectively, I_S and I_R are the integrated emission intensity of the sample and reference respectively, A_S and A_R are the recorded absorbance of the Ruthenium complexes and reference at the excitation wavelength (450 nm) respectively, η_S and η_R are the refractive indices of the solvents used for the sample and reference respectively.

1. H. Ishida, S. Tobita, Y. Hasegawa, R. Katoh and K. Nozaki, Recent advances in instrumentation for absolute emission quantum yield measurements, *Coord. Chem. Rev.*, **2010**, *254*, 2449–2458.
2. J. V. Caspar and T. J. Meyer, Photochemistry of $[Ru(bpy)_3]^{2+}$, *J. Am. Chem. Soc*., **1983**, *105*, 5583–5590.